UTJMS 2025 February 05, **13**(S1):e1-e12 https://doi.org/10.46570/utjms-2025-1359

The effects of the ketone body β-hydroxybutyrate on the neuronal transcriptome

Zayn Cheema[1*], Megan Chen[1*], Dana Poon[1*], Taara Reddy[1*], John Vergis[2], Sinead M. O'Donovan[3]

[1] High School Student, Summer Biomedical Science Program in Bioinformatics, Department of Neurosciences and Psychiatry, University of Toledo, 3000 Arlington Ave, Toledo, OH, 43614

[2]Graduate Student, Department of Neurosciences and Psychiatry, University of Toledo, 3000 Arlington Ave, Toledo, OH, 43614

[3] University Teacher in Advanced Biological Techniques, Department of Biological Sciences, University of Limerick, Castletroy, Limerick, V94 T9PX

[*]Authors contributed equally to this submission.

Email: sinead.odonovan@ul.ie

Received: 2024-08-23

Accepted for publication: 2024-10-23

Published: 05 February 2025

Abstract

The ketogenic diet is emerging as an effective therapeutic option for patients with neurological disorders. The diet results in metabolism of fatty acids to ketone bodies like β-hydroxybutyrates (BHBs), which serve as an alternative fuel source for brain cells. However, the molecular effect of BHB on neurons is not well understood. We hypothesized that BHB administration will induce upregulation of energy metabolism-related processes in neurons. To assess the effect of BHB administration on the neuronal transcriptome, we reanalyzed a publicly available RNAseq dataset (GSE252513) using a bioinformatic "3-pod" approach. We conducted pathway analysis and identified leading edge genes using Gene Set Enrichment Analysis (GSEA) and conducted chemical perturbagen analysis using the iLINCS repository to identify drugs that are concordant and discordant with BHB administration. We identified significantly altered ($p<0.05$) pathways associated with inflammation and immunity such as "regulation of proinflammatory cytokine production" and "modulation of inflammatory responses." We did not identify significant modulation of energy metabolism-related pathways in response to BHB administration. Our results suggest that under normal conditions, BHBs primary actions include modulation of cellular neuronal immune responses.

Keywords: Neuron, Transcriptome, Ketone Body

1. Introduction

The brain is an energy demanding organ. Neurons use a significant proportion (over 75%) of the brain's energy supply, to facilitate signaling-related processes including the maintenance of resting membrane potential, generation of action potentials, and synaptic transmission (1). Neuronal function may be affected in central nervous system (CNS) disorders that are associated with energy metabolism deficits (2). Adenosine triphosphate

(ATP) is the brain's principal energy currency. It is generated through the process of glycolysis in the cytosol and by oxidative phosphorylation in mitochondria (3). When glucose availability is low, the liver produces ketone bodies, which are water soluble molecules produced by the metabolism of fatty acids (4). The two primary types of ketone bodies are acetoacetate (AcAc) and, the focus of our study, β-hydroxybutyrate (BHB). Ketone body generation begins in the hepatic mitochondria, where fatty acids are broken down into acetyl-CoA. While some of this acetyl-CoA is funneled through the Kreb's cycle and ultimately used in the generation of ATP, the excess is used for ketogenesis. Ketone bodies which are produced through ketogenesis are released into the bloodstream where they are taken up by cells of the CNS, including neurons (5). The ketone bodies are metabolized to acetyl-CoA in the brain cell's mitochondria and used in the generation of cellular ATP, thus supplying energy sourced from fats rather than sugar (6). The ketogenic diet is a high-fat, low-carbohydrate diet that supplies the body with fatty acids as an alternative to glucose. It shows promise for the treatment of CNS disorders.

In an assessor-blinded trial studying the role of the ketogenic diet in Alzheimer's patients, significant improvements were seen in the Activities of Daily Living and Quality of Life scale, a commonly used instrument to assess Alzheimer's disease patients (7). Patients with neuropsychiatric disorders including bipolar disorder reported clinical benefits after following the ketogenic diet for 2-3 years, allowing them to discontinue the use of lamotrigine medication. Those same patients saw improved Quality of Life scores (8). Acute administration of the ketogenic diet also results in overall symptom improvement in patients with bipolar disorder. Approximately 70% of bipolar disorder patients on a 4-month ketone diet had a greater than one point improvement on the Clinical Global Scale (9). Patients with other CNS disorders also show benefits from the ketogenic diet. In patients with autism, the ketogenic diet improves social-behavioral deficits, communication, and repetitive behavior patterns (10). Childhood epilepsy patients reported significant improvements following administration of the ketogenic diet; 38% of children had a 50% seizure reduction compared to only 6% of children in the control group (11). Studies have also explored whether the ketogenic diet, which can be unpalatable for patients, is necessary to induce these therapeutic benefits or if administering ketone bodies (BHBs) alone can have the same therapeutic effect. The effect of BHB administration alone was investigated in a mouse model of epilepsy. BHB suppressed inflammatory responses and thus, BHB was proposed as a potential treatment for epilepsy due to its neuroprotective effects (12).

Ketone bodies have shown positive effects when studied in people with neurodevelopmental and neurodegenerative diseases (13). The presence of BHB plays a vital role in keeping the brain's neurons healthy. The mechanisms by which BHB contributes to maintaining brain health are an important area of study. Impaired glucose metabolism is reported in many CNS disorders (14). Providing the brain with ketones, such as with the ketogenic diet, may provide an alternative source of ATP production in the brain by supplying ketones through fatty acid oxidation (15). Although earlier studies considered the need for glucose starvation in combination with supply of ketone bodies, supplementing the brain's energy supply with BHB may potentially overcome the energy deficits associated with these disorders, leading to improvement of symptoms. Anti-epileptic treatments were reduced during dietary intervention in a case study of a subject with autism in her adolescent years (10). At puberty, the subject developed seizures and was treated with a gluten free, casein-free ketogenic diet. This resulted in high ketosis. The ketogenic diet reduced her seizures, weight, and autism symptoms (10). This raises the question, could BHB be a leading factor in these results?

In addition to its role as an energy source, BHB also modulates inflammation. BHB has significant effects on the enzyme histone deacetylase (HDAC). HDAC catalyzes the deacetylation of histones and is involved in the epigenetic regulation of inflammatory gene expression (16). BHB is a specific inhibitor of HDACs (17). When HDAC activity is impaired, it leads to increased inflammation in the brain (18). BHB administration restored histone deacetylation in a murine model of Huntington's disease (19). BHB induces ramification of the brain's primary immune cells, microglia, promoting anti-inflammatory effects. BHB administration increases anti-inflammatory

cytokine IL-10 expression via AKT signaling (20). HDAC inhibition also induces similar changes in microglial ramification (20), suggesting that BHB anti-inflammatory activity is mediated by its role as an endogenous HDAC inhibitor. Studying the effects of BHB is pertinent to CNS disorders as a growing body of studies show its therapeutic potential. The underlying mechanisms of BHBs therapeutic effects are still unclear. Thus, in this study we address the effects of administering BHB on human neurons. We hypothesize that BHB treated neurons will display significant changes in 1) energy metabolism related gene expression and 2) immune related gene expression. We test our hypothesis by reanalyzing a published RNAseq dataset using our bioinformatic "3-pod" approach.

2. Methods

RNAseq data was generated as described in Nomura et.al (21). Raw RNAseq (fastq) files were downloaded from the Gene Expression Omnibus (GSE252513). Briefly, human neurons (ScienCell) cultured in neuron media (ScienCell) were administered 10 µM BHB (Sigma Aldrich) and harvested at 24 hours for RNA extraction and RNAseq analysis (21). Control group neurons were cultured in neuron media with no addition of BHB (**Figure 1**).The experiment was conducted using n=3 replicates for each group. For data analysis, the aligned RNAseq reads were analyzed for differential expression between BHB treated cells and controls. Differential expression analysis was performed using the R programming language (22) with edgeR dependencies limma (23) and voom (24); covariates were ignored due to a lack of data provided in the Gene Expression Omnibus entry. Any genes which did not have corresponding HGNC symbols were removed from the analysis. Duplicate genes were combined using the mean of the log2 fold change (log2FC) and the maximum of the p-value, ensuring a conservative approach to the data. Following this, the resultant differentially expressed gene list was submitted to a three-prong analysis including gene set enrichment analysis (GSEA) (25) and iLINCS analysis (26). The resulting pathways were clustered using Pathway Analysis Visualization with Embedding Representations (PAVER) (27). The 3-pod workflow (https://doi.org/10.5281/zenodo.8190833) is described in Figure 1. Venn diagrams and heatmaps used to visualize shared clusters or pathways were generated by the 3-pod bioinformatic workflow.

3. Results

In total, 4,822 genes were significantly differentially expressed ($p \leq 0.05$) in BHB-treated neurons compared to neurons in the control group (**Figure 2**). GDF15 is a gene that regulates food intake, energy expenditure, and body weight. The upregulation of this gene is associated with disease states like inflammation, injury, and oxidative stress. Immune-related pathway clusters were significantly enriched in BHB-treated neurons compared to controls (**Figure 3**).Upregulated immune-related pathway clusters include pathways associated with positive regulation of cytokine production, positive regulation of leukocyte mediated immunity, regulation of T-cell proliferation, cell-cell adhesion regulation, adaptive immune response, regulation of mononuclear cell migration, regulation of phagocytosis, and response to molecule of bacterial origin. Downregulated enriched pathways following BHB administration are associated with cell division processes and include mitotic sister chromatid segregation, chromosome segregation, and DNA conformation change (**Figure 3)**. Other enriched pathway clusters include those associated with cholesterol metabolism and cellular signaling processes like Wnt signaling and phospholipase C activity. Energy-metabolism related pathways were not significantly enriched following GSEA analysis. Leading-edge (LE) genes are the genes that are most frequently identified in significant ($p<0.05$) GSEA pathways but are not necessarily significantly differentially expressed.

Overall, the top LE genes (**Figure 4A**) are related to inflammation and immune activity. They include: the chemokine C-C motif chemokine ligand 5 (CCL5), a component in immunoregulatory and inflammatory processes, PYD and CARD domain containing (PYCARD), which is involved in the activation of the inflammasome, annexin A1 (ANXA1), which is involved in innate immune response and has anti-inflammatory activity and interleukin 23 receptor (IL23R), the receptor for the pro-inflammatory cytokine IL23. Many of the bottom

10 LE genes (**Figure 4B**) are involved in cell division processes. Polo like kinase 1 (PLK1) is related to mitosis and downregulation is associated with inhibited cancer cell growth, APC regulator of WNT signaling pathway (APC) is a tumor suppressor and regulates cell division, zw10 kinetochore protein (ZW10) is associated with cell division checkpoint, aurora kinase B (AURKB) is a serine/threonine kinase involved in mitosis regulation and semaphorin 5A (SEMA5A) is an axonal growth cone guidance protein implicated in neural development. Histone deacetylase (HDAC) genes (**Figure 4C**) were predominantly downregulated, an expected outcome as BHB is a known inhibitor of HDAC enzymes.

Concordant drugs (**Figure 5A**) like HDAC inhibitors play important roles in epigenetic or non-epigenetic regulation, inducing death, apoptosis, and cell cycle arrest in cancer cells (28) which could help treat neurological disorders through their gene regulatory properties. HDAC inhibitors exert an anti-inflammatory effect by modulating the acetylation of both histone and non-histone proteins, which alters the expression of inflammatory genes and pathways, though their precise role can vary depending on the specific cell type and inflammatory stimulus (29). CDK inhibitors block the production of CDK enzymes, which are partially responsible for cell division; because of this, increased CDK inhibitors may decrease the risk of cancer and other neurological diseases (30). Discordant drugs (Figure 5B) like KIT inhibitors inhibit KIT which can sometimes develop into tumors (31). FLT3 inhibitors, another downregulated drug MoA, reduce neuropathic pain (32). Similarly, PDGFR tyrosine kinase receptor inhibitors are also used to treat tumors as they block receptors that mediate autocrine tumor growth, use fibroblast-rich tumor stroma, and regulate tumor vasculature. KIT inhibitors, FLT3 inhibitors, and PDGFR tyrosine kinase receptor inhibitors each influence blood-brain barrier cell processes by altering receptor signaling pathways that impact tumor growth, neuropathic pain, and tumor vasculature, thereby affecting the cellular interactions and permeability of the blood-brain barrier.

4. Discussion

BHB can keep the brain's neurons healthy and has previously improved various neurological conditions. We hypothesized that BHB administration modulates metabolism-related gene expression and immune response in neurons, which may contribute to its therapeutic effects. In order to test this hypothesis, we analyzed a publicly available RNAseq dataset using a “3-pod” bioinformatic workflow to determine the effect of BHB treatment on the transcriptome of human neurons. Surprisingly, we did not identify a significant effect of BHB on energy metabolism in neurons under the studied experimental conditions. However, DEG and LE gene analysis implicated immune-related genes, particularly proinflammatory cytokines and chemokines like CCL5, PYCARD, ANXA1, IL23R, and IL23, following BHB treatment. These genes were predominantly upregulated; interestingly anti-inflammatory related genes like GNG10 were significantly downregulated, suggesting increased immune activation in response to BHB treatment. BHB treatment is a mediator of systemic and brain inflammation (9), but less is known about its role in different cell types. Nomura and colleagues showed that inflammatory gene response is muted in unstimulated, BHB-treated microglia (21). In response to lipopolysaccharide (LPS) administration, inflammatory gene activation is significantly upregulated in untreated cells, but not in BHB-treated microglia. This supports an anti-inflammatory role for BHB following LPS activation but a mild proinflammatory response under other conditions. Our results suggest that neurons respond in a similar manner to microglia under non stimulated conditions as BHB appears to have a proinflammatory effect in our analysis. How neurons respond to a combination of LPS and BHB treatment will form the basis of future studies and will be important to understanding the potential role of BHB in disease conditions. Our results also suggest a potential mechanism for the inflammatory effects of BHB administration. iLINCS analysis identified HDAC inhibitors as drugs that induce gene signatures that are concordant with BHB administration. HDACs are potent regulators of neuroinflammation and HDAC inhibitors are being explored as anti-inflammatory agents for the treatment of CNS disorders (33).

Unsurprisingly, the immune-modulatory effect of HDAC inhibitors is well-studied in microglia. For example, HDAC inhibition drives changes in the functional ramification of microglia to an anti-inflammatory phenotype (34). It has been proposed that BHBs effect on microglial ramification is mediated by HDAC inhibition (20). Interestingly, our results suggest that BHBs immune modulatory effects in neurons may also be mediated via HDAC regulation.

Our initial hypothesis proposed that BHB treatment would induce significant changes in energy metabolism, as BHB is a ketone body that can be used by neurons as an alternative source of fuel. However, we found few pathways related to energy metabolism and mitochondria in our analysis. Further experiments, for example comparing the effects of BHBs on energy metabolism under glucose starvation conditions or under other stressor conditions, will be necessary to determine whether energy substitution is a primary mechanism of BHBs in neurons. Limitations to be considered include the time course of this study. RNAseq data was generated after 24hrs of BHB administration, which can obscure the longer-term effects of BHB with the ephemeral effect of inflammation. The longer-term effects of BHB on the neuronal transcriptome have yet to be studied. Cell culture offers an excellent way to study the effects of BHB directly on human neurons. However, these findings do not necessarily reflect the effects of BHB in the human brain, which is a complex tissue composed of diverse and interdependent neuronal and glial cell types. Overall, our results indicate that BHB-treatment induces significant changes in immune and inflammatory gene expression in neurons.

To date, studies about BHBs effects on neurons largely focused on its role as an energy substrate but our study suggests that changes in bioenergetic processes is not a major effect of acute BHB administration. This is reflected by the data, as the primary DEG, pathway and LE findings are predominantly linked to immune response. While BHBs role as a systemic and brain immune modulator are established, much less is known about its effect on neurons specifically. Our results reveal further insight into this topic. We found BHB has mild proinflammatory effects on neurons under normal growth conditions. Our data suggests that these immune effects may be regulated via BHBs action as a mediator of HDACs. As for future applications, these findings suggest BHB administration as a possible method for regulating inflammation in neurons and support further exploration of this ketone body in the treatment of neurological disorders.

5. Conflicts

The authors have no conflicts to declare.

6. References

1. Engl, E. and D. Attwell, *Non-signalling energy use in the brain.* J Physiol, 2015. **593**(16): p. 3417-29.

2. Duarte, J.M., P.F. Schuck, G.L. Wenk and G.C. Ferreira, *Metabolic disturbances in diseases with neurological involvement.* Aging Dis, 2014. **5**(4): p. 238-55.

3. Dunn, J. and M.H. Grider, *Physiology, Adenosine Triphosphate*, in *StatPearls*. 2024: Treasure Island (FL).

4. Laffel, L., *Ketone bodies: a review of physiology, pathophysiology and application of monitoring to diabetes.* Diabetes Metab Res Rev, 1999. **15**(6): p. 412-26.

5. Dhillon, K.K. and S. Gupta, *Biochemistry, Ketogenesis*, in *StatPearls*. 2024: Treasure Island (FL).

6. Puchalska, P. and P.A. Crawford, *Multi-dimensional Roles of Ketone Bodies in Fuel Metabolism, Signaling, and Therapeutics.* Cell Metab, 2017. **25**(2): p. 262-284.

7. Phillips, M.C.L., L.M. Deprez, G.M.N. Mortimer, D.K.J. Murtagh, S. McCoy, R. Mylchreest, L.J. Gilbertson, K.M. Clark, P.V. Simpson, E.J. McManus, J.E. Oh, S. Yadavaraj, V.M. King, A. Pillai, B. Romero-Ferrando, M. Brinkhuis, B.M. Copeland, S. Samad, S. Liao and J.A.C. Schepel, *Randomized crossover trial of a modified ketogenic diet in Alzheimer's disease.* Alzheimers Res Ther, 2021. **13**(1): p. 51.

8. Phelps, J.R., S.V. Siemers and R.S. El-Mallakh, *The ketogenic diet for type II bipolar disorder.* Neurocase, 2013. **19**(5): p. 423-6.

9. Sethi, S., D. Wakeham, T. Ketter, F. Hooshmand, J. Bjornstad, B. Richards, E. Westman, R.M. Krauss and L. Saslow, *Ketogenic Diet Intervention on Metabolic and Psychiatric Health in Bipolar and Schizophrenia: A Pilot Trial.* Psychiatry Res, 2024. **335**: p. 115866.

10. Herbert, M.R. and J.A. Buckley, *Autism and dietary therapy: case report and review of the literature.* J Child Neurol, 2013. **28**(8): p. 975-82.

11. Neal, E.G., H. Chaffe, R.H. Schwartz, M.S. Lawson, N. Edwards, G. Fitzsimmons, A. Whitney and J.H. Cross, *The ketogenic diet for the treatment of childhood epilepsy: a randomised controlled trial.* Lancet Neurol, 2008. **7**(6): p. 500-6.

12. Si, J., Y. Wang, J. Xu and J. Wang, *Antiepileptic effects of exogenous beta-hydroxybutyrate on kainic acid-induced epilepsy.* Exp Ther Med, 2020. **20**(6): p. 177.

13. Jensen, N.J., H.Z. Wodschow, M. Nilsson and J. Rungby, *Effects of Ketone Bodies on Brain Metabolism and Function in Neurodegenerative Diseases.* Int J Mol Sci, 2020. **21**(22).

14. Arvanitakis, Z., R.S. Wilson, J.L. Bienias, D.A. Evans and D.A. Bennett, *Diabetes mellitus and risk of Alzheimer disease and decline in cognitive function.* Arch Neurol, 2004. **61**(5): p. 661-6.

15. Rho, J.M., *How does the ketogenic diet induce anti-seizure effects?* Neurosci Lett, 2017. **637**: p. 4-10.

16. Rao, R., W. Fiskus, S. Ganguly, S. Kambhampati and K.N. Bhalla, *HDAC inhibitors and chaperone function.* Adv Cancer Res, 2012. **116**: p. 239-62.

17. Shimazu, T., M.D. Hirschey, J. Newman, W. He, K. Shirakawa, N. Le Moan, C.A. Grueter, H. Lim, L.R. Saunders, R.D. Stevens, C.B. Newgard, R.V. Farese, Jr., R. de Cabo, S. Ulrich, K. Akassoglou and E. Verdin, *Suppression of oxidative stress by beta-hydroxybutyrate, an endogenous histone deacetylase inhibitor.* Science, 2013. **339**(6116): p. 211-4.

18. Lim, S., A.S. Chesser, J.C. Grima, P.M. Rappold, D. Blum, S. Przedborski and K. Tieu, *D-beta-hydroxybutyrate is protective in mouse models of Huntington's disease.* PLoS One, 2011. **6**(9): p. e24620.

19. Alam, M.M., M. Chattopadhyaya and S. Chakrabarti, *Solvent induced channel interference in the two-photon absorption process--a theoretical study with a generalized few-state-model in three dimensions.* Phys Chem Chem Phys, 2012. **14**(3): p. 1156-65.

20. Huang, C., P. Wang, X. Xu, Y. Zhang, Y. Gong, W. Hu, M. Gao, Y. Wu, Y. Ling, X. Zhao, Y. Qin, R. Yang and W. Zhang, *The ketone body metabolite beta-hydroxybutyrate induces an antidepression-associated ramification of microglia via HDACs inhibition-triggered Akt-small RhoGTPase activation.* Glia, 2018. **66**(2): p. 256-278.

21. Nomura, M., N.F. Murad, S.S. Madhavan, B. Eap, T.Y. Garcia, C.G. Aguirre, E. Verdin, L. Ellerby, D. Furman and J.C. Newman, *A ketogenic diet reduces age-induced chronic neuroinflammation in mice Running title: ketogenic diet and brain inflammaging.* bioRxiv, 2024.

22. Love, M.I., S. Anders, V. Kim and W. Huber, *RNA-Seq workflow: gene-level exploratory analysis and differential expression.* F1000Res, 2015. **4**: p. 1070.

23. Liu, S., Z. Wang, R. Zhu, F. Wang, Y. Cheng and Y. Liu, *Three Differential Expression Analysis Methods for RNA Sequencing: limma, EdgeR, DESeq2.* J Vis Exp, 2021(175).

24. Costa-Silva, J., D. Domingues and F.M. Lopes, *RNA-Seq differential expression analysis: An extended review and a software tool.* PLoS One, 2017. **12**(12): p. e0190152.

25. Subramanian, A., P. Tamayo, V.K. Mootha, S. Mukherjee, B.L. Ebert, M.A. Gillette, A. Paulovich, S.L. Pomeroy, T.R. Golub, E.S. Lander and J.P. Mesirov, *Gene set enrichment analysis: a knowledge-based approach for interpreting genome-wide expression profiles.* Proc Natl Acad Sci U S A, 2005. **102**(43): p. 15545-50.

26. Evangelista, J.E., D.J.B. Clarke, Z. Xie, A. Lachmann, M. Jeon, K. Chen, K.M. Jagodnik, S.L. Jenkins, M.V. Kuleshov, M.L. Wojciechowicz, S.C. Schurer, M. Medvedovic and A. Ma'ayan, *SigCom LINCS: data and metadata search engine for a million gene expression signatures.* Nucleic Acids Res, 2022. **50**(W1): p. W697-W709.

27. Ryan, V.W., A.S. Imami, H. Ali Sajid, J. Vergis, X. Zhang, J. Meller, R. Shukla and R. McCullumsmith, *Interpreting and visualizing pathway analyses using embedding representations with PAVER.* Bioinformation, 2024. **20**(7): p. 700-704.

28. Kim, H.J. and S.C. Bae, *Histone deacetylase inhibitors: molecular mechanisms of action and clinical trials as anti-cancer drugs.* Am J Transl Res, 2011. **3**(2): p. 166-79.

29. Adcock, I.M., *HDAC inhibitors as anti-inflammatory agents.* Br J Pharmacol, 2007. **150**(7): p. 829-31.

30. Zhang, M., L. Zhang, R. Hei, X. Li, H. Cai, X. Wu, Q. Zheng and C. Cai, *CDK inhibitors in cancer therapy, an overview of recent development.* Am J Cancer Res, 2021. **11**(5): p. 1913-1935.

31. Klug, L.R., C.L. Corless and M.C. Heinrich, *Inhibition of KIT Tyrosine Kinase Activity: Two Decades After the First Approval.* J Clin Oncol, 2021. **39**(15): p. 1674-1686.

32. Rivat, C., C. Sar, I. Mechaly, J.P. Leyris, L. Diouloufet, C. Sonrier, Y. Philipson, O. Lucas, S. Mallie, A. Jouvenel, A. Tassou, H. Haton, S. Venteo, J.P. Pin, E. Trinquet, F. Charrier-Savournin, A. Mezghrani, W. Joly, J. Mion, M. Schmitt, A. Pattyn, F. Marmigere, P. Sokoloff, P. Carroll, D. Rognan and J. Valmier, *Inhibition of neuronal FLT3 receptor tyrosine kinase alleviates peripheral neuropathic pain in mice.* Nat Commun, 2018. **9**(1): p. 1042.

33. Dai, Y., T. Wei, Z. Shen, Y. Bei, H. Lin and H. Dai, *Classical HDACs in the regulation of neuroinflammation.* Neurochem Int, 2021. **150**: p. 105182.

34. Wang, G., Y. Shi, X. Jiang, R.K. Leak, X. Hu, Y. Wu, H. Pu, W.W. Li, B. Tang, Y. Wang, Y. Gao, P. Zheng, M.V. Bennett and J. Chen, *HDAC inhibition prevents white matter injury by modulating microglia/macrophage polarization through the GSK3beta/PTEN/Akt axis.* Proc Natl Acad Sci U S A, 2015. **112**(9): p. 2853-8.

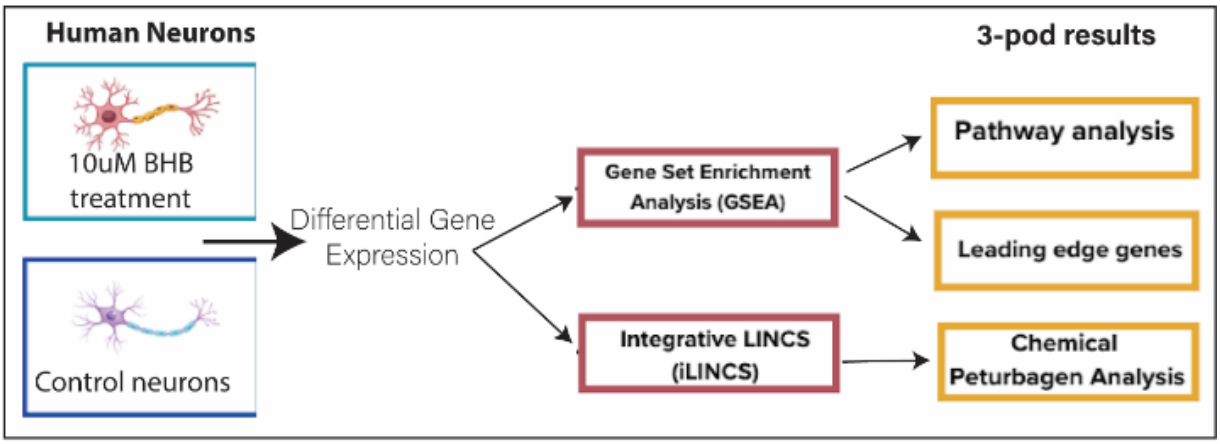

Figure 1. Experiment and bioinformatic analysis workflow.

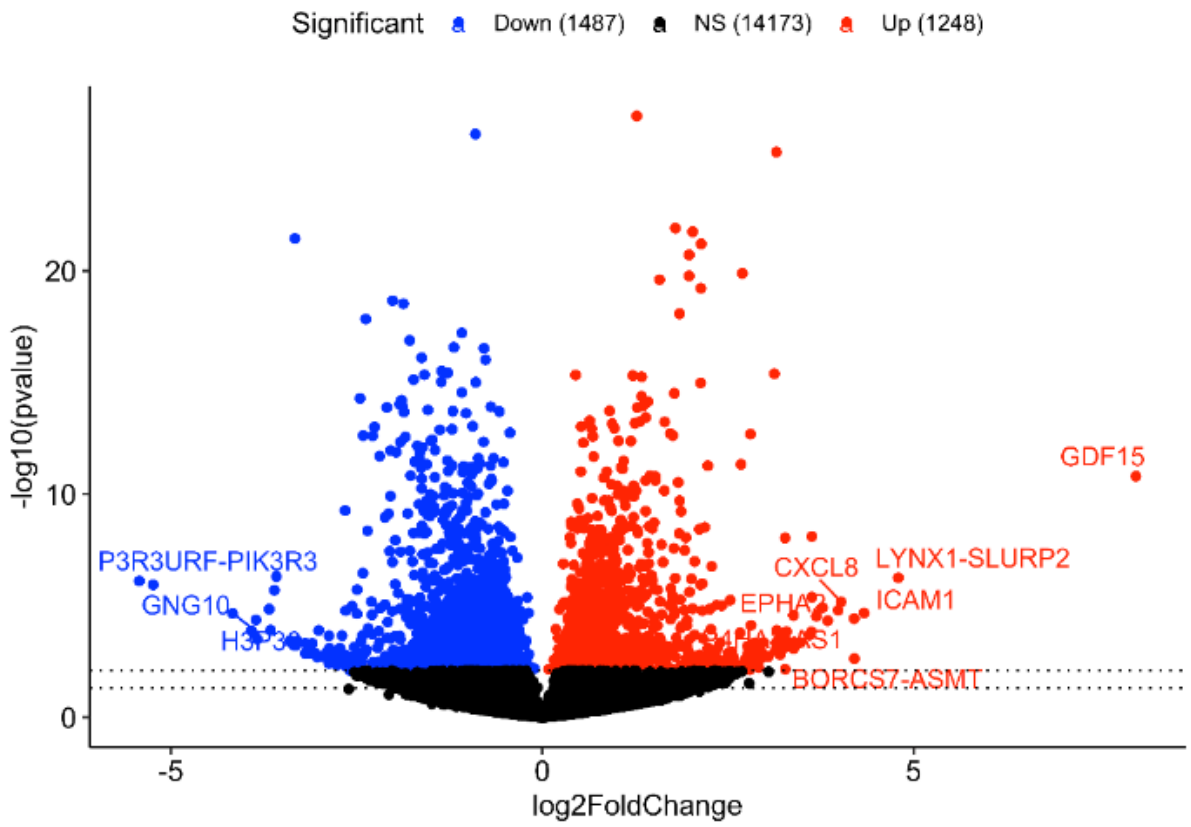

Figure 2. RNAseq analysis of β-hydroxybutyrate (BHB)-treated primary human neurons. Data are expressed as a volcano plot of log2 fold change (x-axis) and -log10 (p-value) (y-axis). Positive values (red dots) indicate genes with significantly increased expression, while negative values (blue dots) indicate genes with significantly decreased expression. The first dotted line (from bottom to top) indicates an unadjusted threshold of significance $p \leq 0.05$, whereas the second dotted line above the first one indicates an adjusted threshold of significance, adjusted $p \leq 0.05$. Annotated genes are those which were both significant by their p-value after adjustment for multiple testing and were the top 10 genes with the greatest absolute log-fold change, defining them as the "most" differentially expressed genes found in the dataset.

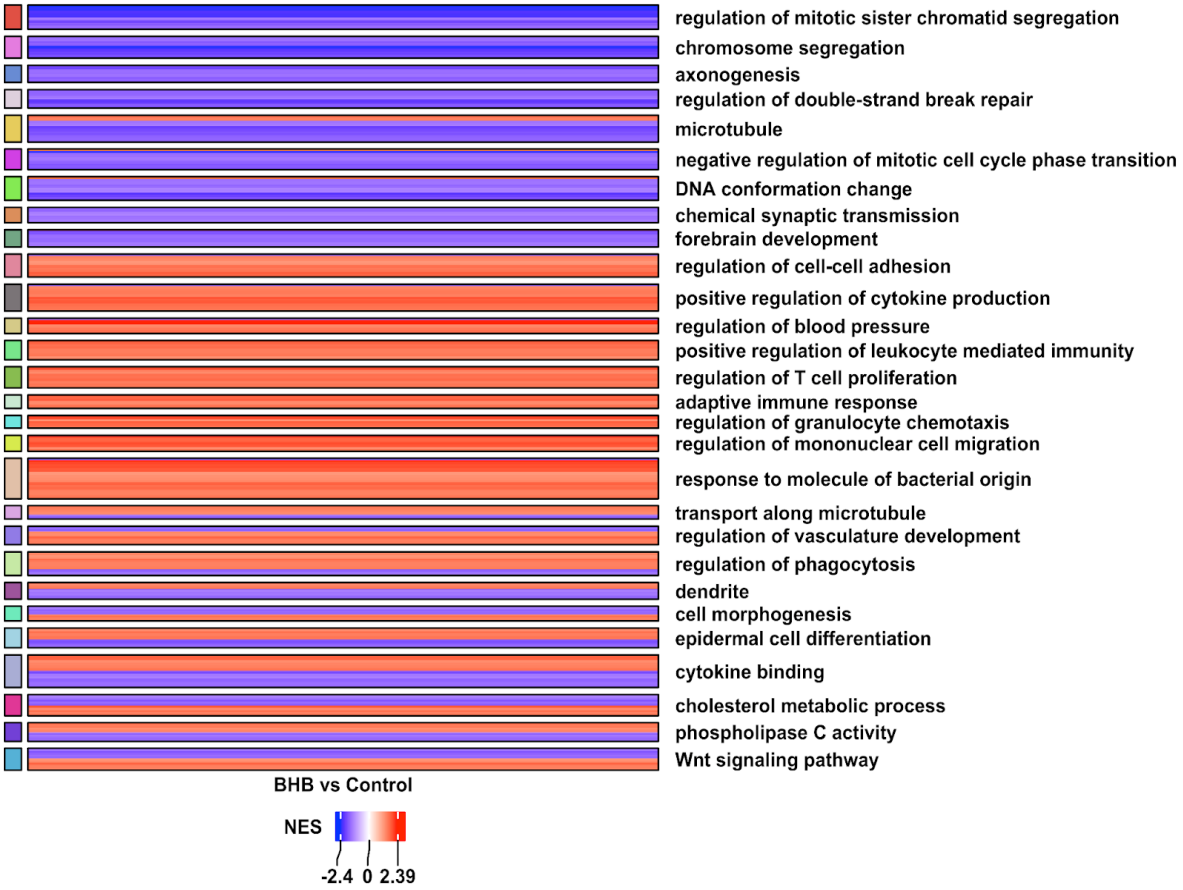

Figure 3. Heatmap of gene set enrichment analysis (GSEA) identifying differentially expressed pathways ($p \leq 0.05$). Cluster analysis was conducted using PAVER. Pathways are presented by normalized enrichment score (NES). A positive NES (red) indicates over-represented or enriched pathways in BHB treated neurons. A negative NES indicated pathway under-representation in BHB treated neurons.

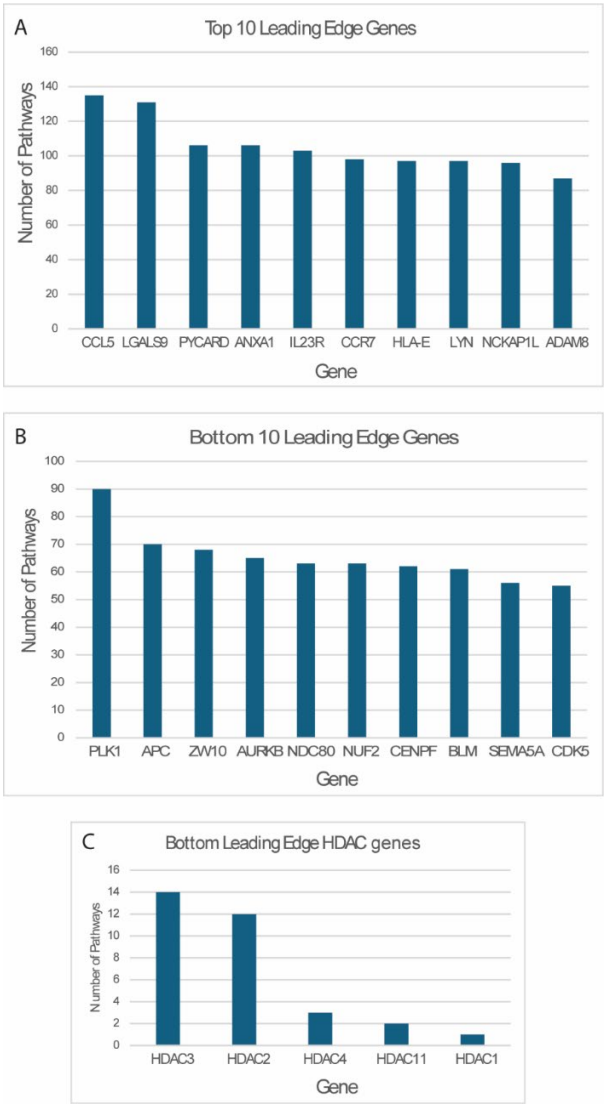

Figure 4. The top (A) and bottom (B) leading edge (LE) genes in β-hydroxybutyrate (BHB)-treated primary neurons were identified by gene set enrichment analysis (GSEA). Several histone deacetylases (HDAC1- 4, 11) genes were also identified in LE gene analysis in downregulated biological pathways (C). LE genes are the genes that are most frequently identified in significant ($p \leq 0.05$) GSEA pathways but are not necessarily significantly differentially expressed. Data represented on column graphs by LE gene symbol (x-axis) and number of genes (y-axis).

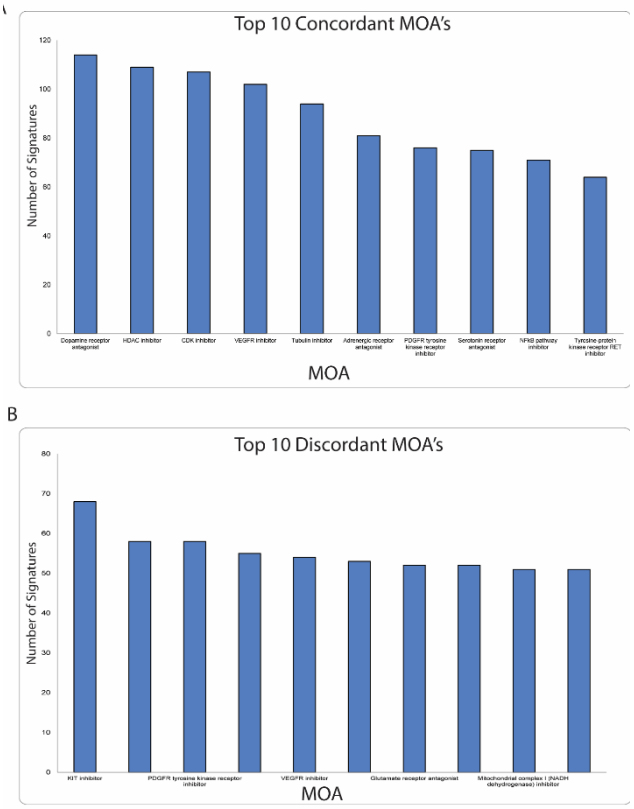

Figure 5. (A) The top mechanisms of action (MoAs) for drugs that induce a gene expression signature similar (concordant) to the gene expression induced by BHB are dopamine receptor antagonists, HDAC inhibitors, and CDK inhibitors. (B) The top MoAs of drugs that induce a gene expression signature that are dissimilar (discordant) to BHB are KIT inhibitors, FLT3 inhibitors, and PDGFR tyrosine kinase receptor inhibitors.

UTJMS 2025 February 05, **13**(S1):e1-e19 https://doi.org/10.46570/utjms-2025-1362

Low dose deltamethrin exposure affects gene expression in rat frontal cortex

Junze Wu[1*], Ariv Shah[1*], Rami Ridi[1*], Zacharia Rashid[1*], Nilanjana Saferin[2], Ali Sajid Imami[3], James Patrick Burkett[4]

[1]High School Student, Summer Biomedical Science Program in Bioinformatics, Department of Neurosciences, College of Medicine and Life Sciences, University of Toledo, Toledo, OH 43614, USA
[2]Undergraduate Student, Department of Neurosciences, College of Medicine and Life Sciences, University of Toledo, Toledo, OH 43614, USA
[3]Department of Neurosciences, University of Toledo, Toledo, OH 43614, USA
[4]Assistant Professor, Department of Neurosciences, University of Toledo, Toledo, OH 43614, USA
[*]Authors contributed equally to the submission.

Email: ali.imami@rockets.utoledo.edu

Received: 2024-08-25

Accepted for publication: 2024-10-16

Published: 05 February 2025

Abstract

Pyrethroids are a class of commonly used synthetic insecticides, widely used in agricultural and residential settings due to their efficacy and relatively low environmental impact. Nonetheless, epidemiological studies have found that exposure to pyrethroids during developmental stages is linked to risk for neurodevelopmental disorders. However, the molecular mechanisms behind these neurotoxic effects remain unclear. Our study investigates the impact of oral exposure to deltamethrin, a widely used Type II pyrethroid pesticide, on gene expression in the frontal cortex of rats. We used differential gene expression data from frontal cortex dissections from male Long-Evans rats exposed to a 3 mg/kg oral dose of deltamethrin (or vehicle) to perform a 3Pod analysis in R Studio, which included GSEA, Enrichr, and iLINCS analyses. We found that rats who were exposed to deltamethrin had significant changes in gene expression in cortex in pathways related to inflammation, apoptosis, cellular energy metabolism, and synapses. Our study provides important insight on the effects of pesticide exposure on the brain and possible treatments and preventions. This study also emphasizes the need for further research on pyrethroid pesticides and their relationship to neurodevelopmental disorders.

Keywords: pyrethroids, pesticides, exposure science, neurotoxicology

1. Introduction

1.1. Pyrethroid Pesticides. Pyrethroid pesticides are synthetic chemicals widely used in agricultural, public, and residential settings, because of their low toxicity and rapid environmental degradation (1). These compounds are also found in household insecticides, pet sprays, shampoos, lice treatments, mosquito repellents, and scabies treatments. They have consistently held a 15%

share of the global market over several decades (2), with an average annual production of 7,000 tons worldwide. Pyrethroids are present in various environmental compartments, including crops, surface water, soil, and air (3, 4). Recent epidemiological data show that the primary metabolite of several pyrethroids (including deltamethrin), 3-phenoxybenzoic acid, is detected in urine at a rate of 78.1% among adults in the USA (5). Deltamethrin is one kind of Type II pyrethroid pesticide extensively used in agriculture, domestic settings, public spaces, and medical applications (6). Deltamethrin is also effective against mosquitoes (7), is recommended by the World Health Organization for this purpose (8) and is widely used for mosquito control in areas where mosquito-borne illnesses are a public health concern. Its presence is common worldwide, significantly boosting crop yields (9). Deltamethrin's impact on the world is substantially large, from increasing public health to supporting the agricultural economy.

1.2. Deltamethrin Risks. Despite its countless benefits, deltamethrin has also raised concerns due to its increasing usage and potential implications for neurodevelopmental disorders (10). Multiple recent epidemiology studies have shown that exposure to pyrethroid pesticides during pregnancy is a risk factor for autism and other neurodevelopmental disorders (11, 12). This finding is supported by laboratory research, including studies in which rats given 3 mg/kg of deltamethrin orally had behavioral and neurological changes relevant to neurodevelopmental disorders, including autism and ADHD (13-16). These studies point to the critical need for additional research into the molecular effects of deltamethrin exposure on the brain.

1.3. Toxicology. In this study, we will examine the effects of an orally administered dose (3 mg/kg) of deltamethrin on gene expression in the frontal cortex of rats, using data generated in an earlier study (17) and accessed through the Gene Expression Omnibus (GEO) database (18). The study used an oral route of exposure, modeling the most common way humans are chronically exposed to deltamethrin and other similar pyrethroids (19). The relevance of the 3 mg/kg dose of deltamethrin lies in its relation to preexisting and well-established benchmarks. The EPA-set benchmark dose (lower confidence limit) for oral exposure to deltamethrin used for regulatory guidance is 10.1 mg/kg, well above the dose used in this study. The "no observable adverse effect limit" (NOAEL) for oral exposure to deltamethrin relative to acute effects on mobility, as identified in some studies (20), is 1.0 mg/kg, just below the 3 mg/kg dose. These two boundaries make the study's 3 mg/kg dose within an area of uncertainty that has a potential for adverse effects but is still well below than the benchmark dose.

1.4. Hypothesis. To further investigate the effect of deltamethrin on brain function, we examined the effects of acute deltamethrin exposure on gene expression profiles from male rat frontal cortex using a previously published dataset. We used innovative bioinformatics approaches to assess gene pathway and network level changes to compare the gene expression in the frontal cortex of rats acutely exposed to deltamethrin versus vehicle controls. We hypothesize that there is a difference in the gene expression in the frontal cortex of deltamethrin exposed rats versus the control rats.

2. Materials and Methods

2.1. Data access. The workflow for this project is outlined in Figure 1. We accessed a dataset from the NCBI GEO database (GSE7955) containing data from a study that investigated the impact of the pyrethroid pesticide deltamethrin on gene transcription in rat frontal cortex (17). The data was accessed on June 24, 2024. The gene count data was downloaded from the GEO website using GEOquery (v 2.66.0) (21). All samples except for

the control and deltamethrin-treated (3 mg/kg dose) groups were excluded from the analysis.

2.2. Animal subjects. All animal subjects were treated, the subsequent biological samples obtained, and microarray transcriptomics performed, as described in the referenced publication (17). Briefly, the researchers in the study exposed male Long-Evans rats to deltamethrin (3 mg/kg via oral gavage, N=8) or vehicle (N=12), euthanized the rats at a 6-hour time point, and dissected frontal cortex samples for use in transcriptomics.

2.3. Differential Gene Expression. Differential gene expression analysis was performed on the gene count data using the limma (v3.54.0) R package (22). As in the source study (17), no covariates were used.

2.4. 3Pod Report. The output of the differential gene expression analysis was used as the input for the 3Pod R script (version 3400184) (23). The 3Pod report was generated on June 25, 2024 (Supplemental File 1). The 3Pod script produces a 3Pod Report that includes the Gene Set Enrichment Analysis (GSEA) (24), Enrichr (25, 26), Library of Integrated Network-based Cellular Signatures (LINCS), and Pathway Analysis Visualization with Embedding Representations (PAVER) (27) analyses listed below. All figures and tables were derived from the 3Pod Report.

2.4.1. GSEA. We analyzed the differential gene expressions using Gene Set Enrichment Analysis (GSEA) (24). GSEA compares a list of genes to gene sets in a compatible database and generates normalized enrichment scores (NES), with positive NES corresponding to "upregulated" gene sets and negative NES corresponding to "downregulated" gene sets. 3Pod used the output of differential gene expression analysis as input to the GSEA and compared this input to the most recent version of the "Enrichment Map Gene Sets" combined database for rat (28) at the time of report generation. The subsequently identified gene sets were placed on the "Upregulated" list (positive NES) or "Downregulated" list (negative NES) and sorted by raw p-value.

2.4.2. Enrichr. Enrichr is a web application that compares a list of genes to a database of gene set libraries and generates Combined Scores (CS) identifying gene sets that are significantly enriched for the listed genes (25, 26). 3Pod used the top 90% and bottom 10% of differentially expressed genes by fold change as input into EnrichR and restricted EnrichR to the Gene Ontology libraries. The subsequently identified gene sets were placed on the "Upregulated" or "Downregulated" list and sorted by raw p-value.

2.4.3. iLINCS. The Integrative Library of Integrated Network-based Cellular Signatures (iLINCS) is a web platform that allows us to compare the differential gene expression signature of a dataset with a large LINCS database of transcriptomic signatures and to generate a similarity score (29). 3Pod used the output of differential gene expression analysis as input into iLINCS and restricted iLINCS to the "LINCS chemical perturbagen signatures" database to produce "concordant" perturbagens with similar transcriptomic profiles and "discordant" perturbagens with dissimilar transcriptomic profiles. iLINCS was then used to perform "Mechanism of Action" analysis to identify molecular mechanisms of action shared by concordant and discordant perturbagens, and "Known Targets" analysis to identify known gene targets of the concordant and discordant perturbagens.

2.4.4. PAVER Analysis. The results from GSEA, EnrichR, and iLINCS analyses were separately clustered using Pathway Analysis Visualization with Embedding Representations (PAVER) (27). PAVER organizes the gene sets into hierarchical clusters and assigns each cluster a name using pathway embeddings. 3Pod separately used the gene set lists from GSEA, EnrichR and iLINCS as

input to PAVER, which produced separate cluster plots and heatmap plots for each.

2.4.5. Venn diagram. 3Pod combined the results from GSEA and EnrichR to produce a list of gene sets common to both analyses. First, the GSEA and EnrichR lists of altered gene sets were each reduced to gene sets present in both databases. Then, the two lists were compared, and a Venn diagram was generated showing the total number of commonly altered gene sets. Finally, two tables were generated showing the subset of these commonly altered gene sets that were either upregulated on both lists ("Shared Upregulated") or downregulated on both lists ("Shared Downregulated").

3. Results

3.1. Differential Gene Expression. We performed differential gene expression analysis on a downloaded transcriptomics dataset from an experiment in which rats were exposed acutely to deltamethrin (Fig. 1). The differentially expressed genes in frontal cortex between control and deltamethrin-exposed rats are visualized in the volcano plot (Fig. 2), which include the upregulated genes Nr4a1 (nuclear receptor subfamily 4 group A member 1), Klf2 (KLF transcription factor 2), and Rnf6 (ring finger protein 6), and the downregulated genes Gpd1 (glycerol-3-phosphate dehydrogenase 1), Fkbp5 (FKBP prolyl isomerase 5), and Hspb1 (heat shock protein family B (small) member 1).

3.2. GSEA. GSEA identified 1055 altered gene sets (unadjusted $p<0.05$) in the exposed group as compared to vehicle controls, among which 155 were significant at adjusted $p<0.05$ (Table 1, Supplemental File 1). Of the 1055 identified gene sets, 598 were upregulated and 457 were downregulated. The highest NES for the upregulated pathways corresponded to the "positive regulation of t-cell proliferation" gene set, and the three lowest enrichment scores for the downregulated pathways all related to mitochondrial gene sets. A PAVER heatmap was generated to organize upregulated and downregulated gene sets into identifiable clusters (Fig. 3). The most significant primarily upregulated gene set cluster (in red) was "actin-based cell projections," while the most significant primarily downregulated gene set cluster was "intracellular protein transport."

3.3. EnrichR. EnrichR identified 375 significantly enriched gene sets at an unadjusted $p<0.05$. EnrichR was unable to identify any significant gene sets with adjusted $p<0.05$.

3.4. iLINCS. iLINCS identified 567 transcriptomic signatures in the chemical perturbagen database that were positively correlated with the deltamethrin exposure signature ("concordant perturbagens") and 918 that were negatively correlated ("discordant perturbagens") (Table 2, Supplemental File 1). The top concordant perturbagen that was an identifiable pharmacological agent was Lanacordin, an inhibitor of sodium-potassium ATPase; while the top discordant perturbagen was the pharmacological agent Tanespimycin, an antibiotic that acts to inhibit Heat Shock Protein 90 (HSP90). Mechanism of Action (MOA) analysis identified 246 concordant MOAs and 292 discordant MOAs. The most common concordant MOA was "Cyclin-dependent kinase (CDK) inhibitor," while the most common discordant MOA was "acetylcholine receptor antagonist." iLINCS Known Targets analysis produced no concordant or discordant gene targets that were significant at $p<0.05$.

3.5. GSEA and Enrichr Venn Diagram. The 3Pod report combined the GSEA and Enrichr results, creating a Venn diagram (Fig. 4, Supplemental File 1). The 1055 altered gene sets from GSEA and 375 enriched gene sets from EnrichR were first reduced to 1030 and 369 gene sets, respectively, which appeared in both databases. Among the altered gene sets contained in both databases, the GSEA and EnrichR results shared 44 gene sets in common, of which 26 were upregulated in both

analyses and 12 were downregulated in both analyses. The top 2 shared upregulated pathways were “neuron projection cytoplasm” and “dendrite cytoplasm,” and the top two shared downregulated pathways were “negative regulation of intrinsic apoptotic signaling” and “positive regulation of membrane potential.”

4. Discussion

4.1. To investigate the effects of acute deltamethrin exposure on the brain, we studied a previously existing dataset (17) containing gene expression data from frontal cortex tissue of acutely exposed rats, using advanced bioinformatics methods. Differential gene expression was analyzed and then further examined using 3Pod, which produced the GSEA, Enrichr, iLINCS, and PAVER analyses. We found that frontal cortex from rats who were exposed to deltamethrin had significant changes in gene expression compared to control, especially in gene sets related to inflammation, apoptosis, energy metabolism/mitochondria, and synaptic structure/function.

4.2. Inflammation & Apoptosis. 3Pod analysis revealed a pattern in gene expression changes in the brain caused by exposure to deltamethrin that corresponds to changes in gene sets for inflammation and apoptosis. Apoptosis, also known as programmed cell death, ensures both the removal of damaged neurons and overgrowth of glial cells (30) and is essential for developmental plasticity and organismal health, playing key roles in brain development by aiding cell differentiation, localization, and population control (31). Among the differentially expressed genes, three of the most upregulated by fold change were Nr4a1, Klf2, and Rnf6; and one of the most downregulated was Fkbp5. Nr4a1 is a transcription factor involved in cellular processes like cell cycle mediation, inflammation, and apoptosis, and plays an important role in both cell survival and death (32). An increase in the gene expression of Nr4a1 also signifies more cellular stress and inflammation (33), both contributing to neurodevelopmental conditions like autism spectrum disorder and ADHD (34). Klf2 is also a transcription factor involved in vascular and immune functions in the body (35). An increased expression of Klf2 significantly affects the brain and leads to neuroinflammation, which can lead to an increased risk of neurodevelopmental disorders like autism (36). Rnf6 is a protein-coding involved in protein degradation (37) that also helps maintain protein homeostasis and create signaling pathways. An increase in Rnf6 expression means that the cell has detected and is responding to inflammation (38). GSEA showed the “positive regulation of t-cell proliferation” as the most upregulated gene set. As a part of the immune system, T-cells are a type of white blood cell that helps protect the body from infection by directly killing virus-infected cells or sending signals to trigger a larger immune response. Positive regulation of T-cell proliferation indicates an increase in T-cell production and activity, which could be indicative of an immune response to an inflammatory condition. Fkbp5 codes for a protein in the immunophilin protein family which plays an important role in immunoregulation. It is thought to control calcineurin inhibition, which itself activates T-cells (39). Finally, the Venn diagram of GSEA and EnrichR results shows the “negative regulation of intrinsic apoptotic signaling pathway” was downregulated in both analyses, indicating a disinhibition of apoptotic signaling.

4.3. Cellular Energy & Metabolism. Our results show changes in gene expression corresponding to cellular energy and metabolism. Among the differentially expressed genes, one of the most downregulated by fold change was Gpd1. Gpd1 codes for an enzyme crucial in carbohydrate and lipid metabolism (40), which is crucial for energy. A decreased expression could mean less energy available to neurons of the frontal cortex. The animals exposed to deltamethrin were found to move 30% less and have decreased neuronal firing in the frontal cortex (17). GSEA also revealed

numerous downregulated gene sets related to mitochondrial function, including the three most significantly downregulated gene sets, "mitochondrial protein-containing complex," "mitochondrial inner membrane," and "mitochondrial ribosome." Mitochondria are organelles responsible for generating cellular energy in the form of adenosine triphosphate (ATP). The mitochondrial protein-containing complex can refer to components of the electron transport chain (ETC) and ATP synthase. Downregulation of mitochondrial protein-containing complexes leads to impaired energy production because of reduced ATP levels (41). Similarly, the inner mitochondrial member separates mitochondria into two regions and is the working space of the ETC, which is responsible for oxidative phosphorylation. Mitochondrial ribosomes are also active in the ETC (42). Neurons are very demanding in ATP, so a downregulation of three important functions in the mitochondria can severely impact brain function.

4.4. Brain Development. PAVER analysis of the GSEA gene sets showed multiple dysregulated gene set clusters related to synaptic function, including "cluster of actin-based cell projections," "postsynaptic membrane," "monoatomic anion channel activity," and "cell surface receptor signaling pathway." Actin-based cell projections are structures that extend from the surface of a cell rich in cytoskeleton protein actin. Actin-based cell projections are important for the development of both dendrites and their dendritic spines (43), which are essential structural components of neuronal transmission (44). The combined GSEA and Enrichr gene sets also support our hypothesis that deltamethrin impacts pathways relevant to brain development, as there is a shared upregulation of the "neuron projection cytoplasm" and "dendrite cytoplasm" gene sets. Dynamic changes in dendrites and dendritic spines are often significant in brain development and a disruption in those dynamics can lead to neurodevelopmental disorders, including autism spectrum disorder (45). GSEA analysis also showed gene expression changes related to intracellular protein transport. Proteins are synthesized in ribosomes, which are then transported in vesicles between different organelles (46). A downregulation in intracellular protein transport can impact brain development as well. Certain proteins participate in neurotransmission and synapse function. Disruption in protein transport in these areas can harm synapses and their function, which are important for memory and learning (47). There are also proteins that assist in the development of neurons, therefore a downregulation in transport could adversely affect brain development.

4.5. Lanacordin & Tanespimycin. Perturbagen analysis identified specific chemicals that have both similar and dissimilar effects to deltamethrin exposure in frontal cortex. In our study, we found that Lanacordin treated cells showed a gene expression pattern highly similar to deltamethrin exposure. This means that the drug mimics the effect of deltamethrin on cells. Lancordin, commonly referred to as digoxin, is a cardiac glycoside prescribed to treat heart problems and known for its cardiotoxic effects (48). Lanacordin's mechanism of action involves inhibiting the sodium potassium pump (49). Lanacordin impacts neuronal function by disrupting cellular ion homeostasis, which is critical for neuronal membrane potentials (50) . This can lead to changes in excitability and action potentials, leading to neurological side effects such as confusion, memory impairment, hallucinations, and delirium (51). Tanespimycin, whose transcriptional profile had a high dissimilarity with deltamethrin exposure, serves as an antineoplastic agent and apoptosis inducer (52). Tanespimycin's mechanism of action is the inhibition of heat shock protein 90 (Hsp90), which is crucial in function and stability of proteins involved in cell growth by coupling with the ubiquitination pathway (53, 54).

4.6. iLINCS CDK inhibitor/iLINCS acetylcholine receptor antagonist. The mechanism of action shared by the most drugs on the concordant perturbagen list was “cyclin-dependent kinase (CDK) inhibitor.” The function of CDK inhibitors is to prevent the activities of CDKs during the cell cycle (55, 56). Exposure to the pyrethroid β-cypermethrin can downregulate both the protein expression levels of CDK4, CDK6, and mRNA expression levels of p21 and cyclin3, all of which contribute to the cell cycle (57). CDK4 is particularly involved in controlling the progression of cells from the G1 phase to S phase. Downregulation and inhibitors of this may halt the cell cycle, leading to a delay in cell division and cell growth (56). Disruptions in CDK4 functioning have also been associated with neurodevelopmental disorders (58). Although more research needs to be done, it can be inferred that deltamethrin may directly act as an inhibitor or may facilitate the downregulation of CDK4. The mechanism of action shared by the most drugs on the discordant perturbagen list was “acetylcholine receptor antagonist.” Acetylcholine receptors are critical cholinergic signaling molecules important for neuronal signaling, particularly in learning and memory (59). This disruption in acetylcholine signaling is particularly relevant to neurodevelopmental disorders, as proper functioning of acetylcholine receptors is essential for normal brain development and function (60).

5. Limitations

Our study involves several limitations that impact the depth and interpretation of our findings. The primary limitation on our findings is the use of an extensive range of exploratory bioinformatics techniques. These methods are very robust in generating new hypotheses, but the ability to conclusively determine statistical significance is limited by the number of analyses run and the number of hypotheses tested by each. This is amplified by the use of unadjusted p-values by some analyses in 3Pod, as either the input, the output, or both. Additionally, the selection of a previously analyzed dataset from the GEO database makes this study subject both to selection bias and to the authors’ foreknowledge of some existing differences. Another major limitation is the reliance on a single time point to assess gene expression dynamics following exposure to deltamethrin. Gene expression can vary significantly over time following acute exposure to a toxicant, influencing the observed outcomes (61). Incorporating multiple time points throughout the exposure and recovery phases could have helped in capturing more dynamic changes in gene expression patterns. Finally, the original study which was the source of the data analyzed here had several key limitations. First, the use of an animal model, and also the use of only male subjects, limits the generalizability of any results derived from the experiment. A second limitation of the original study, published in 2008, is that the gene count data was collected using a slightly outdated microarray technique instead of RNA-Seq. While microarrays offer a broad survey of gene expression patterns, RNA-Seq offers more differentially expressed protein coding genes, more toxicological and biological insight, and overall, it identifies more differentially expressed genes (62).

6. Conclusion

Using the 3Pod report containing Enrichr, LINCS, GSEA, and PAVER analyses, we were able to support the idea that there is a difference in the gene expression in the frontal cortex of deltamethrin exposed rats compared to the control rats. Deltamethrin exposure produced a wide range of changes in gene expression in genes and gene sets related to inflammation, apoptosis, cellular energy, and brain development. This leads to a wide range of effects on neuronal function that may explain, in part, the known effects of acute deltamethrin exposure on movement (17) and cognitive function (63) and the known effects of chronic developmental exposure on

neurodevelopmental disorder related neurobehavioral phenotypes (13-16). Our findings suggest new hypotheses for molecular mechanisms, new directions for research, and new potential avenues for preventing and reversing the effects of pyrethroid exposure.

7. Data Availability

All sequencing data were downloaded from NCBI GEO (GSE7955) on June 24, 2024. All code used to analyze the data is on GitHub repository CogDisResLab/galaxy1_3podr.

8. Disclosures

The authors declare no conflicts of interest.

9. Author Contributions

JPB and ASI selected the data set, designed the study, and designed the analytic strategy. ASI downloaded the data from the GEO database. JW, AS, RR, and ZR performed background research and participated in data analysis, interpretation of results, and assembly of figures under the guidance of NS, ASI, and JPB. All authors participated in writing the manuscript and approved the final version.

Acknowledgements

We would like to acknowledge the essential role of the Summer Biomedical Science Program in Bioinformatics in organizing, educating, and guiding young researchers to perform research of this kind. This research was supported in part by funding from the NIH to JPB (NIEHS: R00ES027869).

References

1. Chrustek, A., I. Holynska-Iwan, I. Dziembowska, J. Bogusiewicz, M. Wroblewski, A. Cwynar, and D. Olszewska-Slonina, *Current Research on the Safety of Pyrethroids Used as Insecticides.* Medicina (Kaunas), 2018. **54**(4).
2. Stellman, S.D. and J.M. Stellman, *Pyrethroid insecticides—time for a closer look.* JAMA Internal Medicine, 2020. **180**(3): p. 374-375.
3. Tang, W., D. Wang, J. Wang, Z. Wu, L. Li, M. Huang, S. Xu, and D. Yan, *Pyrethroid pesticide residues in the global environment: An overview.* Chemosphere, 2018. **191**: p. 990-1007.
4. Li, H., F. Cheng, Y. Wei, M.J. Lydy, and J. You, *Global occurrence of pyrethroid insecticides in sediment and the associated toxicological effects on benthic invertebrates: an overview.* Journal of hazardous materials, 2017. **324**: p. 258-271.
5. Lehmler, H.-J., D. Simonsen, B. Liu, and W. Bao, *Environmental exposure to pyrethroid pesticides in a nationally representative sample of US adults and children: The National Health and Nutrition Examination Survey 2007–2012.* Environmental Pollution, 2020. **267**: p. 115489.
6. Mestres, R. and G. Mestres, *Deltamethrin: uses and environmental safety.* Rev Environ Contam Toxicol, 1992. **124**: p. 1-18.
7. Kumar, S., A. Thomas, and M. Pillai, *Deltamethrin: Promising mosquito control agent against adult stage of Aedes aegypti L.* Asian Pacific Journal of Tropical Medicine, 2011. **4**(6): p. 430-435.
8. Organization, W.H., *Safety of pyrethroids for public health use*. 2005, World Health Organization.
9. Pulman, D.A., *Deltamethrin: the cream of the crop.* Journal of agricultural and food chemistry, 2011. **59**(7): p. 2770-2772.
10. Pitzer, E.M., M.T. Williams, and C.V. Vorhees, *Effects of pyrethroids on brain development and behavior: Deltamethrin.* Neurotoxicology and teratology, 2021. **87**: p. 106983.
11. Hicks, S.D., M. Wang, K. Fry, V. Doraiswamy, and E.M. Wohlford, *Neurodevelopmental delay diagnosis rates are increased in a region with aerial pesticide application.* Frontiers in pediatrics, 2017. **5**: p. 116.
12. Shelton, J.F., E.M. Geraghty, D.J. Tancredi, L.D. Delwiche, R.J. Schmidt, B. Ritz, R.L. Hansen, and I. Hertz-Picciotto, *Neurodevelopmental disorders and prenatal residential proximity to agricultural pesticides: the CHARGE study.*

Environmental health perspectives, 2014. **122**(10): p. 1103-1109.
13. Richardson, J.R., M.M. Taylor, S.L. Shalat, T.S. Guillot III, W.M. Caudle, M.M. Hossain, T.A. Mathews, S.R. Jones, D.A. Cory-Slechta, and G.W. Miller, *Developmental pesticide exposure reproduces features of attention deficit hyperactivity disorder.* The FASEB Journal, 2015. **29**(5): p. 1960.
14. Curtis, M.A., R.K. Dhamsania, R.C. Branco, J.-D. Guo, J. Creeden, K.L. Neifer, C.A. Black, E.J. Winokur, E. Andari, B.G. Dias, R.C. Liu, S.L. Gourley, G.W. Miller, and J.P. Burkett, *Developmental pyrethroid exposure causes a neurodevelopmental disorder phenotype in mice.* PNAS Nexus, 2023. **2**(4).
15. Nguyen, J.H., M.A. Curtis, A.S. Imami, W.G. Ryan, K. Alganem, K.L. Neifer, N. Saferin, C.N. Nawor, B.P. Kistler, G.W. Miller, R. Shukla, R.E. McCullumsmith, and J.P. Burkett, *Developmental pyrethroid exposure disrupts molecular pathways for MAP kinase and circadian rhythms in mouse brain.* bioRxiv, 2024: p. 2023.08.28.555113.
16. Curtis, M.A., N. Saferin, J.H. Nguyen, A.S. Imami, W.G. Ryan, K.L. Neifer, G.W. Miller, and J.P. Burkett, *Developmental pyrethroid exposure in mouse leads to disrupted brain metabolism in adulthood.* NeuroToxicology, 2024.
17. Harrill, J.A., Z. Li, F.A. Wright, N.M. Radio, W.R. Mundy, R. Tornero-Velez, and K.M. Crofton, *Transcriptional response of rat frontal cortex following acute in vivo exposure to the pyrethroid insecticides permethrin and deltamethrin.* BMC genomics, 2008. **9**: p. 1-23.
18. Edgar, R., M. Domrachev, and A.E. Lash, *Gene Expression Omnibus: NCBI gene expression and hybridization array data repository.* Nucleic acids research, 2002. **30**(1): p. 207-210.
19. Lu, C., D.B. Barr, M.A. Pearson, L.A. Walker, and R. Bravo, *The attribution of urban and suburban children's exposure to synthetic pyrethroid insecticides: a longitudinal assessment.* J Expo Sci Environ Epidemiol, 2009. **19**(1): p. 69-78.
20. Authority, E.F.S., *Review of the existing maximum residue levels for deltamethrin according to Article 12 of Regulation (EC) No 396/2005.* EFSA Journal, 2015. **13**(11): p. 4309.
21. Davis, S. and P.S. Meltzer, *GEOquery: a bridge between the Gene Expression Omnibus (GEO) and BioConductor.* Bioinformatics, 2007. **23**(14): p. 1846-1847.
22. Ritchie, M.E., B. Phipson, D. Wu, Y. Hu, C.W. Law, W. Shi, and G.K. Smyth, *limma powers differential expression analyses for RNA-sequencing and microarray studies.* Nucleic acids research, 2015. **43**(7): p. e47-e47.
23. Ryan, W., *willgryan/3PodR_bookdown: Pre-release for Zenodo DOI (pre-release).* Zenodo, 2023.
24. Subramanian, A., P. Tamayo, V.K. Mootha, S. Mukherjee, B.L. Ebert, M.A. Gillette, A. Paulovich, S.L. Pomeroy, T.R. Golub, E.S. Lander, and J.P. Mesirov, *Gene set enrichment analysis: a knowledge-based approach for interpreting genome-wide expression profiles.* Proc Natl Acad Sci U S A, 2005. **102**(43): p. 15545-50.
25. Chen, E.Y., C.M. Tan, Y. Kou, Q. Duan, Z. Wang, G.V. Meirelles, N.R. Clark, and A. Ma'ayan, *Enrichr: Interactive and collaborative HTML5 gene list enrichment analysis tool.* BMC Bioinformatics, 2013. **14**: p. 128.
26. Xie, Z., A. Bailey, M.V. Kuleshov, D.J.B. Clarke, J.E. Evangelista, S.L. Jenkins, A. Lachmann, M.L. Wojciechowicz, E. Kropiwnicki, K.M. Jagodnik, M. Jeon, and A. Ma'ayan, *Gene Set Knowledge Discovery with Enrichr.* Curr Protoc, 2021. **1**(3): p. e90.
27. Ryan V, W.G., A.S. Imami, H. Eby, J. Vergis, X. Zhang, J. Meller, R. Shukla, and R. McCullumsmith, *Interpreting and visualizing pathway analyses using embedding representations with PAVER.* Bioinformation, 2024. **20**(7): p. 700-704.
28. Merico, D., R. Isserlin, O. Stueker, A. Emili, and G.D. Bader, *Enrichment map: a network-based method for gene-set enrichment visualization and interpretation.* PLoS One, 2010. **5**(11): p. e13984.
29. Pilarczyk, M., M.F. Najafabadi, M. Kouril, J. Vasiliauskas, W. Niu, B. Shamsaei, N. Mahi, L. Zhang, N. Clark, Y. Ren, S. White, R. Karim, H. Xu, J. Biesiada, M.F. Bennet, S. Davidson, J.F.

Reichard, V. Stathias, A. Koleti, D. Vidovic, D.J.B. Clark, S. Schurer, A. Ma'ayan, J. Meller, and M. Medvedovic, *Connecting omics signatures of diseases, drugs, and mechanisms of actions with iLINCS.* bioRxiv, 2019: p. 826271.
30. Roth, K.A. and C. D'Sa, *Apoptosis and brain development.* Mental retardation and developmental disabilities research reviews, 2001. **7**(4): p. 261-266.
31. Anosike, N.L., J.F. Adejuwon, G.E. Emmanuel, O.S. Adebayo, H. Etti-Balogun, J.N. Nathaniel, O.I. Omotosho, M. Aschner, and O.M. Ijomone, *Necroptosis in the developing brain: role in neurodevelopmental disorders.* Metabolic Brain Disease, 2023. **38**(3): p. 831-837.
32. Ipseiz, N., S. Uderhardt, C. Scholtysek, M. Steffen, G. Schabbauer, A. Bozec, G. Schett, and G. Krönke, *The nuclear receptor Nr4a1 mediates anti-inflammatory effects of apoptotic cells.* The Journal of Immunology, 2014. **192**(10): p. 4852-4858.
33. Moriyama, K., A. Horino, K. Kohyama, Y. Nishito, T. Morio, and H. Sakuma, *Oxygen–Glucose Deprivation Increases NR4A1 Expression and Promotes Its Extranuclear Translocation in Mouse Astrocytes.* Brain Sciences, 2024. **14**(3): p. 244.
34. Jeanneteau, F., C. Barrère, M. Vos, C.J. De Vries, C. Rouillard, D. Levesque, Y. Dromard, M.-P. Moisan, V. Duric, and T.C. Franklin, *The stress-induced transcription factor NR4A1 adjusts mitochondrial function and synapse number in prefrontal cortex.* Journal of Neuroscience, 2018. **38**(6): p. 1335-1350.
35. Jha, P. and H. Das, *KLF2 in regulation of NF-κB-mediated immune cell function and inflammation.* International journal of molecular sciences, 2017. **18**(11): p. 2383.
36. Eissa, N., A. Sadeq, A. Sasse, and B. Sadek, *Role of neuroinflammation in autism spectrum disorder and the emergence of brain histaminergic system. Lessons also for BPSD?* Frontiers in pharmacology, 2020. **11**: p. 886.
37. Hu, J., G. Wang, and T. Sun, *Dissecting the roles of the androgen receptor in prostate cancer from molecular perspectives.* Tumor Biology, 2017. **39**(5): p. 1010428317692259.
38. Zhai, D., W. Wang, Z. Ye, K. Xue, G. Chen, S. Hu, Z. Yan, Y. Guo, F. Wang, and X. Li, *QKI degradation in macrophage by RNF6 protects mice from MRSA infection via enhancing PI3K p110β dependent autophagy.* Cell & Bioscience, 2022. **12**(1): p. 154.
39. Fries, G.R., N.C. Gassen, and T. Rein, *The FKBP51 glucocorticoid receptor co-chaperone: regulation, function, and implications in health and disease.* International journal of molecular sciences, 2017. **18**(12): p. 2614.
40. Gaertner, K., M. Terzioglu, C. Michell, R. Tapanainen, J.L. Pohjoismäki, E. Dufour, and S. Saari, *A species difference in glycerol-3-phosphate metabolism reveals metabolic adaptations in hares.* bioRxiv, 2024: p. 2024.04.02.587662.
41. Lane, N. and William F. Martin, *The Origin of Membrane Bioenergetics.* Cell, 2012. **151**(7): p. 1406-1416.
42. Ahmad, M., A. Wolberg, and C.I. Kahwaji, *Biochemistry, electron transport chain.* 2018.
43. Wang, W. and M. Rui, *Advances in understanding the roles of actin scaffolding and membrane trafficking in dendrite development.* Journal of Genetics and Genomics, 2024.
44. Belian, S., O. Korenkova, and C. Zurzolo, *Actin-based protrusions at a glance.* Journal of Cell Science, 2023. **136**(22): p. jcs261156.
45. Khanal, P. and P. Hotulainen, *Dendritic Spine Initiation in Brain Development, Learning and Diseases and Impact of BAR-Domain Proteins.* Cells, 2021. **10**(9): p. 2392.
46. Hirokawa, N. and R. Takemura, *Molecular motors in neuronal development, intracellular transport and diseases.* Current opinion in neurobiology, 2004. **14**(5): p. 564-573.
47. Okerlund, N.D. and B.N. Cheyette, *Synaptic Wnt signaling—a contributor to major psychiatric disorders?* Journal of neurodevelopmental disorders, 2011. **3**: p. 162-174.
48. Patocka, J., E. Nepovimova, W. Wu, and K. Kuca, *Digoxin: Pharmacology and toxicology—A review.* Environmental toxicology and pharmacology, 2020. **79**: p. 103400.

49. Zhao, S., X. Li, W. Wu, S. Liu, M. Shen, Z. Zhang, and J. He, *Digoxin reduces the incidence of prostate cancer but increases the cancer-specific mortality: a systematic review and pooled analysis.* Andrologia, 2021. **53**(11): p. e14217.
50. Cao, J., D. Yao, R. Li, X. Guo, J. Hao, M. Xie, J. Li, D. Pan, X. Luo, and Z. Yu, *Digoxin ameliorates glymphatic transport and cognitive impairment in a mouse model of chronic cerebral hypoperfusion.* Neuroscience Bulletin, 2022: p. 1-19.
51. Van Tonder, J.J., *Effect of the cardiac glycoside, digoxin, on neuronal viability, serotonin production and brain development in the embryo*. 2008: University of Pretoria (South Africa).
52. Erlichman, C., *Tanespimycin: the opportunities and challenges of targeting heat shock protein 90.* Expert opinion on investigational drugs, 2009. **18**(6): p. 861-868.
53. Modi, S., A. Stopeck, H. Linden, D. Solit, S. Chandarlapaty, N. Rosen, G. D'Andrea, M. Dickler, M.E. Moynahan, and S. Sugarman, *HSP90 inhibition is effective in breast cancer: a phase II trial of tanespimycin (17-AAG) plus trastuzumab in patients with HER2-positive metastatic breast cancer progressing on trastuzumab.* Clinical Cancer Research, 2011. **17**(15): p. 5132-5139.
54. Taldone, T., A. Gozman, R. Maharaj, and G. Chiosis, *Targeting Hsp90: small-molecule inhibitors and their clinical development.* Current opinion in pharmacology, 2008. **8**(4): p. 370-374.
55. Zhang, M., L. Zhang, R. Hei, X. Li, H. Cai, X. Wu, Q. Zheng, and C. Cai, *CDK inhibitors in cancer therapy, an overview of recent development.* American journal of cancer research, 2021. **11**(5): p. 1913.
56. Goel, S., M.J. DeCristo, S.S. McAllister, and J.J. Zhao, *CDK4/6 inhibition in cancer: beyond cell cycle arrest.* Trends in cell biology, 2018. **28**(11): p. 911-925.
57. Zhou, Y.-J., Y.-Q. Geng, R.-F. Gao, X.-Q. Liu, X.-M. Chen, and J.-L. He, *Early pregnancy exposure to beta-cypermethrin compromises endometrial decidualisation in mice via downregulation of cyclin D3, CDK4/6, and p21.* Food and Chemical Toxicology, 2022. **169**: p. 113382.
58. Khadem-Reza, Z.K. and H. Zare, *Evaluation of brain structure abnormalities in children with autism spectrum disorder (ASD) using structural magnetic resonance imaging.* The Egyptian Journal of Neurology, Psychiatry and Neurosurgery, 2022. **58**(1): p. 135.
59. Hasselmo, M.E., *The role of acetylcholine in learning and memory.* Current Opinion in Neurobiology, 2006. **16**(6): p. 710-715.
60. Oz, M., L.A. Kury, B. Sadek, and M.O. Mahgoub, *The role of nicotinic acetylcholine receptors in the pathophysiology and pharmacotherapy of autism spectrum disorder: Focus on α7 nicotinic receptors.* The International Journal of Biochemistry & Cell Biology, 2024. **174**: p. 106634.
61. Heijne, W.H., A.S. Kienhuis, B. van Ommen, R.H. Stierum, and J.P. Groten, *Systems toxicology: applications of toxicogenomics, transcriptomics, proteomics and metabolomics in toxicology.* Expert Rev Proteomics, 2005. **2**(5): p. 767-80.
62. Rao, M.S., T.R. Van Vleet, R. Ciurlionis, W.R. Buck, S.W. Mittelstadt, E.A.G. Blomme, and M.J. Liguori, *Comparison of RNA-Seq and Microarray Gene Expression Platforms for the Toxicogenomic Evaluation of Liver From Short-Term Rat Toxicity Studies.* Frontiers in Genetics, 2019. **9**.
63. Pitzer, E.M., C. Sugimoto, G.A. Gudelsky, C.L. Huff Adams, M.T. Williams, and C.V. Vorhees, *Deltamethrin Exposure Daily From Postnatal Day 3–20 in Sprague-Dawley Rats Causes Long-term Cognitive and Behavioral Deficits.* Toxicological Sciences, 2019. **169**(2): p. 511-523.

Figures

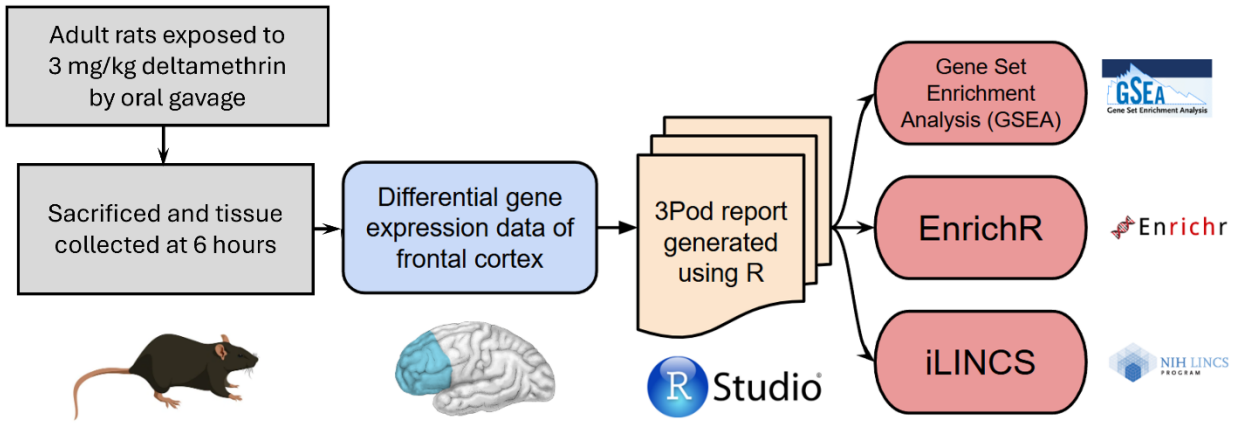

Figure 1. Workflow diagram showing the steps used to perform the exposure, generate data, and analyze the results.

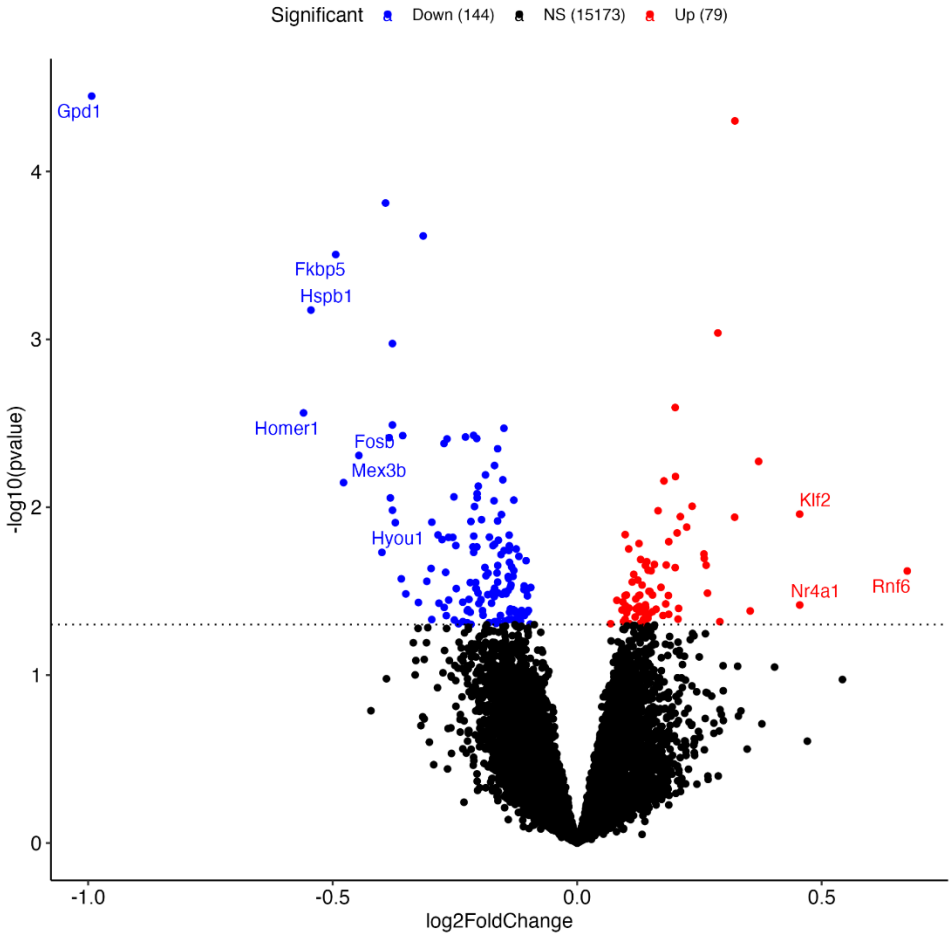

Figure 2. Volcano plot representing the differential gene expression of rats exposed to deltamethrin vs. vehicle controls. The x-axis is the $\log_2$ of the fold change in gene expression for each gene in the dataset, while the y-axis is the inverse $\log_{10}$ of the p-value. Upregulated genes are represented by red circles, and downregulated genes are represented with blue circles. The dotted line is the unadjusted threshold for significance ($p < 0.05$). The annotated genes represent the top differentially expressed genes by fold change.

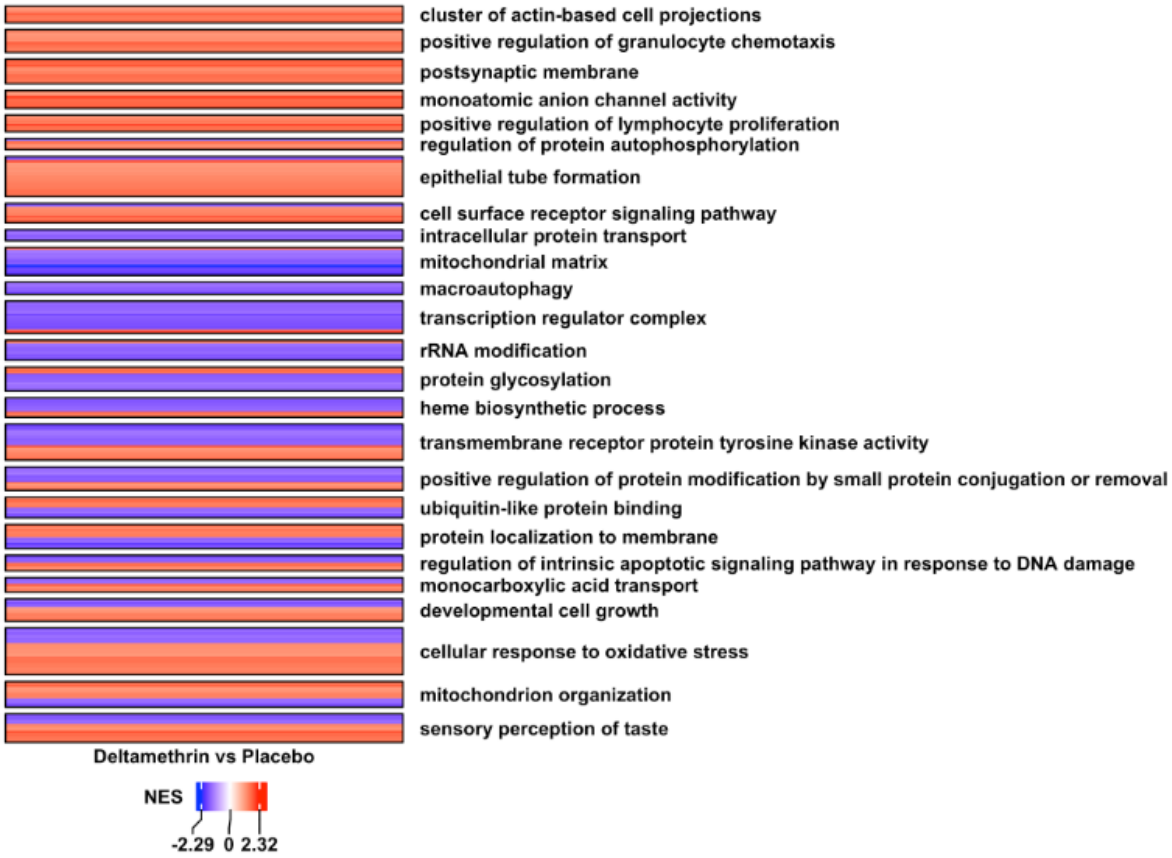

Figure 3. PAVER heatmap showing significant clusters of gene sets from GSEA. Clusters are organized from most significant at the top to least significant at the bottom. Gene sets within the clusters are sorted by normalized enrichment score, with positive scores (upregulated gene sets) shaded in red and negative scores (downregulated gene sets) shaded in blue.

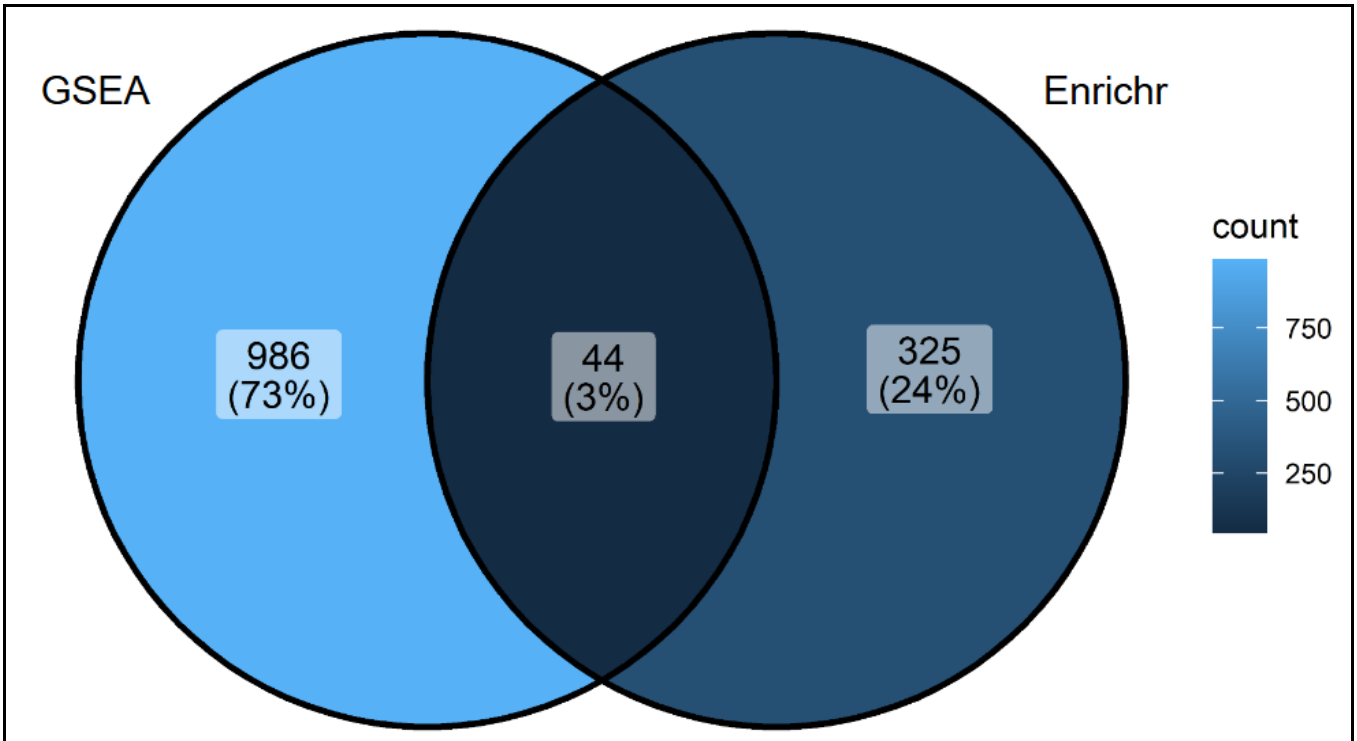

Pathway	GSEA	Enrichr	Pathway	GSEA	Enrichr
Shared Upregulated			**Shared Downregulated**		
neuron projection cytoplasm	1.985	95.32	negative regulation of intrinsic apoptotic signaling pathway	-1.792	-18.58
dendrite cytoplasm	1.862	130.7	positive regulation of membrane potential	-1.538	-18.60
phenol-containing compound biosynthetic process	1.846	95.32	glutamate receptor binding	-1.530	-23.04
catecholamine biosynthetic process	1.805	83.34	response to unfolded protein	-1.495	-5.784
monoatomic anion homeostasis	1.734	110.6	COPI-coated vesicle	-1.483	-23.42
negative regulation of leukocyte chemotaxis	1.624	83.34	G protein-coupled receptor binding	-1.480	-4.524

biogenic amine biosynthetic process	1.623	83.34	phosphoric ester hydrolase activity	-1.474	-4.413
ventricular septum development	1.621	71.49	protein glycosylation	-1.454	-4.134
glucan metabolic process	1.621	130.7	regulation of cell growth	-1.444	-3.271
chloride ion homeostasis	1.580	110.6	negative regulation of protein kinase activity	-1.407	-4.934

Figure 4. Venn diagram illustrating the overlap between results obtained from the GSEA and Enrichr analyses. Color indicates the count of gene sets, with lighter shades representing higher counts. The top 10 upregulated and top 10 regulated pathways are listed and sorted using a combination of GSEA and Enrichr scores.

Pathway	P-value	NES	Pathway	P-value	NES
Upregulated			**Downregulated**		
Positive regulation of t cell proliferation	<0.001	2.321	Mitochondrial protein-containing complex	<0.001	-2.223
Cell surface receptor signaling pathway	<0.001	1.845	Mitochondrial inner membrane	<0.001	-1.938
External side of plasma membrane	<0.001	1.785	Mitochondrial ribosome	<0.001	-2.291
Receptor complex	<0.001	1.743	Organellar ribosome	<0.001	-2.291
Protein complex involved in cell adhesion	0.003	2.207	Organelle inner membrane	<0.001	-1.905
Multicellular organismal process	0.003	1.928	Ribosomal subunit	<0.001	-2.096
Side of membrane	0.003	1.508	Endoplasmic reticulum protein-containing complex	0.001	-2.053
Chloride transport	0.004	1.933	Mitochondrial envelope	0.001	-1.667
Response to ketone	0.007	1.538	Mitochondrial matrix	0.001	-1.821
Cell adhesion mediated by integrin	0.008	2.199	Mitochondrial large ribosomal subunit	0.001	-2.209

Table 1. Gene Set Enrichment Analysis showing the top up-regulated and down-regulated gene sets in exposed samples as compared to vehicle control. NES: Normalized Enrichment Score.

Perturbagen	Similarity	Perturbagen	Similarity
Concordant Signatures		**Discordant Signatures**	
BRD-K30126976	0.417	13-Hydroxy-8,14,19-T**	-0.471
6,10,10B-T*	0.366	Tanespimycin	-0.463
BRD-K86048057	0.365	BRD-K61341215-004-01-2	-0.455
Lanacordin	0.364	NVP-AUY922	-0.441
179324-69-7	0.361	MLS000718723	-0.434
Gossypol	0.358	BRD-K10010115	-0.419
Sepantronium	0.358	Mirin	-0.398
Niclosamide	0.358	PX 12	-0.393
Trichostatin A, Streptomyces Sp.	0.352	CHEMBL2139070	-0.392
BRD-A24396574-001-01-5	0.343	BIIB 021	-0.385

Table 2. iLINCS chemical perturbagen analysis of transcriptomic signatures. Perturbagens with the highest similarity scores relative to the deltamethrin transcriptomic signature are “concordant” while those with the lowest similarity scores are “discordant.”

*6,10,10B-Trihydroxy-3,4a,7,7,10a-pentamethyl-1-oxo-3-vinyldodecahydro-1H-benzo[f]chromen-5-yl acetate

**13-Hydroxy-8,14,19-Trimethoxy-4,10,12,16-tetramethyl-3,20,22-trioxo-2-azabicyclo[16.3.1]docosa-1(21),4,6,10,18-pentaen-9-yl carbamate

Mechanism of Action	**N**	**Mechanism of Action**	**N**
Concordant		**Discordant**	
CDK inhibitor	54	Acetylcholine receptor antagonist	51
NFkB pathway inhibitor	47	HDAC inhibitor	41
Proteasome inhibitor	38	26S proteasome inhibitor	38
D2-like dopamine receptor antagonist	30	CDK inhibitor	34
Serotonin 2a (5-HT2a) receptor antagonist (Serotonin 2a)	30	PI3K inhibitor	30
Epidermal growth factor receptor inhibitor	29	PDGFR tyrosine kinase receptor inhibitor	28
HDAC inhibitor	28	3’,5’-cyclic phosphodiesterase inhibitor	25
Tyrosine-protein kinase receptor RET inhibitor	27	Equilibrative nucleoside transporter 1 inhibitor	25
GABA receptor antagonist	26	Tyrosine kinase inhibitor	25
Dopamine receptor antagonist	25	VEGFR inhibitor	25

Table 3. iLINCS analysis of concordant and discordant mechanisms of action following deltamethrin exposure. Mechanisms of action were ranked by number of occurrences among the significantly concordant and discordant chemical perturbagens.

UTJMS 2025 February 05, **13**(S1):e1-e13 https://doi.org/10.46570/utjms-2025-1536

Borrelia burgdorferi Tolerance-Associated Changes in Gene Expression of Murine Macrophages

Sophia Chen[1*], Ricki Deng[1*], Anis Hadi[1*], Sara Nandwana[1*], William G. Ryan V[2], John B. Presloid[2], R. Mark Wooten[3]

[1]High School Student, Summer Biomedical Science Program in Bioinformatics, Department of Neurosciences, University of Toledo College of Medicine and Life Sciences, Toledo, OH USA

[2]Graduate Student, Department of Neurosciences, University of Toledo College of Medicine and Life Sciences, Toledo, OH USA

[3]Department of Medical Microbiology and Immunology, University of Toledo College of Medicine and Life Sciences, Toledo, OH USA

[*]Authors contributed equally to the submission.

Email: William.Ryan2@rockets.utoledo.edu

Received: 2024-12-17

Accepted for publication: 2025-01-22

Published: 05 February 2025

Abstract

Lyme disease, caused by the spirochete *Borrelia burgdorferi (Bb)*, is the most prevalent vector-borne disease in the United States. Macrophages, key cellular players in the innate immune response, exhibit diminished functionality over time during *Bb* infection, potentially leading to chronic infection. This study explores the transcriptional changes associated with macrophages that develop tolerance to *Bb*. Using RNA sequencing of murine bone marrow-derived macrophages exposed to *Bb*, we identified differentially expressed genes and dysregulated pathways between productively stimulated and tolerized macrophages. Key findings revealed significant downregulation of type-I interferon signaling and associated immune responses, suggesting mechanisms of immune tolerance. Additionally, connectivity analysis identified potential drug candidates for repurposing to enhance macrophage activity. Our results underscore the complexity of macrophage responses to *Bb* and provide a foundation for future research to develop targeted therapies aimed at modulating immune responses and improving treatment outcomes for Lyme disease patients. Ultimately, these findings offer new insights into the pathogenesis and potential treatment strategies for Lyme disease.

Keywords: *Borrelia burgdorferi*, Lyme disease, macrophage, tolerance, transcriptional profiling, drug discovery

1. Introduction

1.1. Overview of Lyme Disease

First documented in Lyme, Connecticut, Lyme disease is an infectious disease caused by the spirochetal bacteria *Borrelia burgdorferi* (*Bb*). The bacterium is spread to humans through the bite of Ixodes ticks, most commonly found in the northeastern and north central regions of the United States (2). A notable symptom to identify

Lyme disease is an erythema migrans skin rash in the shape of a bullseye that emanates from the tick bite site and is sufficient for diagnosis of a *Bb* infection in endemic areas. Other notable but less obvious acute symptoms include fatigue, headache, and fever (2). Even after antibiotic treatments that eventually clear the bacteria, symptoms of the disease can persist. These patients may continue to feel extreme fatigue, muscle pain, and have trouble thinking and performing daily tasks.

1.2. Health Impacts of Lyme Disease

Lyme disease has an estimated 500,000 cases per year in the United States, making it by far the most common vector-borne disease (3). Two different presentations of Lyme disease are diagnosed: acute and chronic. Acute disease has milder symptoms, with symptoms usually disappearing within a week, even without antibiotic treatment. Patients with acute Lyme disease usually make a full recovery if the infection is caught and treated with antibiotic intervention early. However, nearly 20% of patients may go on to develop chronic Lyme disease months later if not appropriately treated. These patients often develop more severe symptoms, including fatigue, muscle aches, arthritis, neurologic deficits, cardiac dysfunction, and increased sensitivity to light and sound (4). Chronic symptoms can continue to persist for many years even after antibiotic treatment, as patients may not experience complete recovery for years. These symptoms have a debilitating impact on a person's daily life. In a case study examining the neurological impacts of chronic Lyme disease symptoms on 24 patients with Lyme disease, 14 of them had memory impairment on neuropsychological tests (5). In 2018, the estimated cost of treating acute Lyme disease in the United States was $4.8 billion, while chronic Lyme disease treatment cost an additional $9.6 billion (6). Patients also reported an estimated cost of $2,000 on average to treat Lyme disease per person (7), showing the financial burden that Lyme disease treatment places on individuals, their families, and the health care system.

1.3. Immune Response to Lyme Disease

After a tick bite, *Bb* enters the dermal tissues of the host. Here, the “first line of defense” of the body is enacted: the innate immune system. The first innate immune cells *Bb* will likely encounter in the dermis are skin-resident macrophages. Macrophages are specialized white blood cells which recognize and scavenge foreign materials, including bacteria such as *Bb* (8). When a macrophage identifies signals that bacteria are present in the system, it will typically migrate to and engulf the bacterium to begin to break it down and kill it. In addition, it secretes soluble mediators that promote the influx of important immune cells from the bloodstream, which are usually needed to completely clear the infection (9).

1.4. Macrophage Tolerance to Bb Clearance

Macrophages use several different receptors and signaling pathways to detect bacteria, including Toll-like receptor 2 (TLR2), the FcγR-receptor and complement receptor-3 (9). When *Bb* enters a host, macrophages sense soluble and surface molecules from the bacterium and move towards it to engulf and kill the *Bb*. However, *Bb* moves at about 10 micrometers per second due to its spirochetal shape and powerful endoflagella, allowing it to move faster than most immune cells, including macrophages (10). In addition to this speed, *Bb* can rapidly sense the environment and change directions, making it incredibly difficult for macrophages and other immune cells to capture the bacteria (11). While macrophages initially appear to efficiently recruit other cells into the area to help clear the infection, over time this recruitment diminishes. A potential explanation for this is that the macrophages are becoming tolerant and no longer recognizing that they need to promote inflammatory responses to clear this infection (1). Thus, while *Bb* is still present in the host, macrophages are no longer acting efficiently to support immune clearance of the persisting bacteria. Therefore, there is great interest in identifying the mechanisms that cause macrophages to cease to efficiently promote immune clearance of *Bb*, so that proper function could be restored and decrease the development of persistent infection and chronic Lyme disease symptoms.

1.5. Transcriptional Assessment of Infection-Induced Mechanisms

Previously, immune tolerance of macrophages in vitro has been studied with enzyme-linked immunosorbent assays (ELISA) by Chung et al. (12). However, the main drawback of sandwich ELISAs is that they usually assess an individual protein target on a particular assay. This means that all other proteins which may be playing a role in infection-induced mechanisms are not assessed. Alternatively, using transcriptional profiling to assess the entire macrophage transcriptome allows for an unbiased analyses of gene regulation (13). The main purposes of this method include diagnosing diseases, planning/creating treatments for diseases, and evaluating how well a treatment is working in some cases (14). In hosts with Lyme disease, we hypothesized that extended exposure to *Bb* causes a subset of macrophage genes to be downregulated, decreasing macrophage functionality to eliminate *Bb*, and therefore creating a tolerance to the infection. Our goal was to elucidate the mechanism(s) within macrophages that suppresses their ability to clear the bacteria by testing macrophage response to single versus multiple stimulations of *Bb* using RNA sequencing (RNAseq). Here, we analyzed differential gene expression using previously collected RNAseq datasets in control and experimental groups of mouse-derived macrophages treated in vitro with and without *Bb* (1).

2. Methods

2.1. Macrophage Isolation and Treatment

This work was performed previously as described by Petnicki-Ocwieja et al. (1) (**Figure 1**). All experiments were approved by Tufts Institutional and Animal Care Committee. Macrophages were expanded from the bone marrow of wild-type mice (C57BL/6J), which are known as marrow-derived macrophages (BMDMs). Briefly, bone marrow was dissociated into 100 mm x 15 mm Petri dishes with sterile DMEM containing 30% L929 cell conditioned medium as the growth factor medium, 20% FBS, and 1% penicillin-streptomycin for 5-7 days, which generates BMDMs. Six plates with 2 x 106 BMDMs each were separated into three groups (n=2): one control and two experimental groups stimulated with *Bb* (B31 or N40 strains). The control group contained unstimulated BMDMs as a baseline comparison. The second group was co-cultured with *Bb* for 6 hours, which represents the initial response of macrophages to *Bb* stimulation during infection (i.e. "stimulated"). The third group was comprised of BMDMs stimulated for 24 hours with *Bb*, washed, then restimulated with *Bb* for 6 hours, representing the responses of macrophages which have had a previous encounter with *Bb* (i.e. "re-stimulated" or "tolerized").

2.2. Generation of RNAseq Library

Macrophage responses were observed by measuring gene expression with RNAseq after 0, 6, and 30 (24+6) hours post-treatment (GSE236149) as described above. After treating harvested cells with TRIzol, libraries were prepared using reagents by Genewiz Inc and sequenced with Illumina HiSeq 4000 at an estimated 25 million reads per sample. Using STAR, the RNAseq reads were aligned to the mm10 mouse reference genome, and RSEM was used to quantify the reads. Differential gene expression analyses were conducted in R using edgeR and voomLmFit. Genes having a FDR-adjusted p-value of < 0.05 were considered significant.

2.3. Bioinformatics Analyses

Our study used a publicly-available R programming language software package (3PodReports) to analyze the publicly collected gene expression data sets (1), which included the gene symbols, log2FoldChange, p-value, and adjusted p-value. 3PodR generates a HTML-format interactive web report, including the results of pathway analyses like Gene Set Enrichment Analysis (GSEA), and computational drug discovery analyses were performed using iLINCS (**Figure 1**) (15-17). Pathways having an FDR adjusted p-value of < 0.05 were considered significant and clustered into biological themes with PAVER (18).

3. Results

3.1. Bb-Mediated Activation vs Tolerance-Associated Gene Expression Signatures

A heatmap depicting the combined top 50 upregulated and downregulated genes by absolute log2 fold change in both the stimulated (6 hr) vs. control (C) groups and the restimulated (24 hr) vs. stimulated (6 hr) groups are shown in **Figure 2A** and **Table S1**.

For the initial activation of macrophages by *Bb* (6hr vs. control groups), the heatmap indicated large numbers of upregulated genes and a smaller subset of downregulated genes. Notable genes in this upregulated group include IL-12α and β, IL-6, CD69, IL-1α, and many other proinflammatory cytokines that have been previously identified to be upregulated by macrophages when exposed to *Bb* in vitro (10). Alternatively, in the macrophages that were restimulated to elicit *Bb*-induced tolerance (24 hr vs. 6 hr groups), analysis shows a much larger subset of downregulated genes compared to upregulated genes. Many of these significantly downregulated genes are the same inflammatory genes that were significantly upregulated in the *Bb*-stimulated populations. Plotting log2 fold change vs log p value allows construction of volcano plots to identify specific genes with significant differences in regulation. Among the stimulated groups vs unstimulated controls, families of inflammatory mediators are significantly upregulated, including interleukins, chemokines and chemokine receptors, and interferon-activated genes (**Figure 2B**).

Conversely, comparing restimulated to stimulated groups, notable genes such as Slpi, Susd2, and Adh7 are significantly upregulated, while downregulated genes include Ngp, Kif18b, and Gm42742 (**Figure 2C**).

3.2. Unsupervised Pathway Clustering Identifies Specific Interferon Dysregulation

Our Gene Set Enrichment Analysis (GSEA) was performed to get a more systems-level assessment of these changes under stimulatory vs tolerance-induced populations. For the 6hr vs control group, a total of 816 significantly altered pathways were identified. Of these 816 pathways, 699 were significantly upregulated while 117 were significantly downregulated. Some of the top upregulated pathways include defense response to other organisms, response to bacteria, and regulation of response to pathogenic stimuli. Some of the top downregulated pathways include cilium, DNA repair, and cilium organization (**Figure 3, Table S2, Table 1**).

A total of 737 significantly altered pathways were identified between the 24hr vs 6hr groups. Of these 737 significant pathways, 173 were significantly up-regulated while 564 were significantly down-regulated. Some of the top upregulated pathways include oxoacid metabolic process, carboxylic acid metabolic process, and organic acid metabolic process. Some of the top down-regulated pathways include inflammatory responses to other organisms, viruses, and other pathogens **(Figure 3, Table S2, Table 1**).

3.3. Connectivity Analysis Identifies Candidate Repurposable Small Molecules

The Library of Integrated Network-based Signatures (LINCS) database was used to identify candidate repurposable drug therapies that potentially could reverse the effect of *Bb*-induced tolerance in macrophages. In our 24hr vs 6hr group, 2368 and 523 L1000 chemical perturbagen signatures in the LINCS database were identified as positively or negatively correlating to our gene signature, respectively (**Table S3**). The top 3 concordant (i.e. positively aligning) perturbagens were PHA-793887, Palbociclib, and Cladribine, while the top 3 discordant (i.e. negatively aligning) perturbagens were SCHEMBL1564574, VU0365118-1, and Parbendazole. We identified a total of 563 unique concordant mechanisms of action (MoA) and 201 unique discordant MoA in the 24hr vs 6hr group. The top MoA for 24hr vs 6hr concordant signatures includes VEGFR inhibitor, PDGFR tyrosine kinase receptor inhibitor and HDAC inhibitor (**Table 2**), while the top MoAs for discordant signatures include tubulin inhibitor, phosphodiesterase inhibitor, and adrenergic receptor agonist (**Table 3**).

In our 6hr vs. Control group, 2960 and 950 L1000 chemical perturbagen signatures in the

LINCS database were identified as positively or negatively correlating to our gene signature, respectively (**Table S4**). The top 3 concordant perturbagens were Nilotinib, Avicin-D, and Oxetane, while the top 3 discordant perturbagens were GSK-3 Inhibitor IX, CHEMBL2143694, and Loperamide. We identified 648 unique concordant MOAs and 273 discordant MOAs. The top 10 concordant MOAs included the dopamine receptor antagonist, VEGFR inhibitor, FLT3 inhibitor, HDAC inhibitor, serotonin receptor antagonist, PDGFR tyrosine kinase receptor inhibitor, CDK inhibitor, glutamine receptor antagonist, KIT inhibitor, and the adrenergic receptor antagonist. Top 10 discordant MOAs included glucocorticoid receptor agonist, acetylcholine receptor antagonist, PI3K inhibitor, adrenergic receptor antagonist, tubulin inhibitor, dopamine receptor agonist, KIT inhibitor, VEGFR inhibitor, PI3-kinase class 1 inhibitor, and PDGFR tyrosine kinase receptor inhibitor.

4. Discussion

4.1. Overview of Research

We investigated the transcriptional changes in macrophages induced by *Bb*, the spirochetal bacterium that caused Lyme disease in humans. Using RNA sequencing along with advanced bioinformatics approaches including STAR, Illumina and edgeR, our study identified differentially expressed genes in macrophages under single (i.e. initial activation; proinflammatory) vs repeated *Bb* stimulations (i.e. induction of tolerance) at optimal times for these conditions. To analyze our gene sequencing results, the R software package 3PodR was used, and key findings reveal that macrophages exhibit a complex transcriptional profile, including both upregulated and downregulated genes, suggesting mechanisms of immune tolerance and inflammation suppression. Using GSEA combined with PAVER, we identified several clusters of pathways with some previously implicated following repeated *Bb* stimulation, including type-1 interferon response and regulation of T cell proliferation, which suggest mechanisms of immune modulation and inflammation suppression in Lyme disease.

4.2. Interferon and Lyme Pathogenesis

Type-I interferon response signaling is one of the strongest correlates with severe cases of Lyme disease Lyme pathogenesis; both patients and/or mouse strains that exhibit severe Lyme-associated pathology display significantly increased production of type-I interferon. *Bb* induces the production of type-I interferon responses (19-21). In general, macrophages produce type-I interferons to defend against bacteria and viruses, particularly those that persist intracellularly. An activated macrophage can produce autocrine or paracrine signaling to neighboring cells to activate or suppress genes, leading to both positive and detrimental effects (22). However, *Bb* can elicit type-I interferon responses that can also lead to further Lyme disease-related complications (23). This is likely counterproductive to clearing these infections, as *Bb* persists extracellularly in dense tissues and mouse models that block type I IFN activation pathways exhibit less severe pathology compared to wild type mice (19). Previous research also shows type-I interferon responses inducing downstream cell signaling pathways when type-I interferons bind to their receptor (IFNAR), and therefore having a significant impact on a variety of biological effects (24).

4.3. Why Macrophages Become Tolerized to Bb

Using GSEA, we selected three genes of interest which were all significantly upregulated: slpi, susd2, and adh (13). Slpi is involved with the immune response, with its best described purpose being protecting epithelial surfaces from bacterial threat using endogenous proteolytic enzymes (25). Susd2 is a gene which is involved in the negative regulation of cell division (26). Adh plays a role in metabolizing a bulk of the ethanol consumed in a diet (27). Using PAVER with GSEA, we identified a cluster of interest, the type-I interferon cluster. Within the type-I interferon cluster, 41 different pathways were identified using transcriptional

profiling. Amongst these, the 3 with the greatest difference in pathway regulation include: positive regulation of cytokine production, positive regulation of interleukin-1 beta production, and regulation of interleukin-1 beta production (**Table 1**). Type-I interferon is known to be a major contributor to the immune response, promoting antiviral effects in multiple non-immune and immune cell types, as well as in the development of CD4+ T cells (28, 29). As shown in Figure 3, the regulation of type-I interferon production is significantly decreased, indicating a correlation between type-I interferon and macrophage response to *Bb*. Since type-I interferon is being downregulated significantly, innate cells are lacking activation signals and T-cells are not developing as needed, which could explain the decrease in macrophage responses since certain T-cells types would likely lack activation in response to chronic *Bb* infection.

5. Conclusion

Our study provides significant insights into the transcriptional changes in macrophages induced by *Bb* and highlights the role of type-I interferon in modulating immune responses during Lyme disease, both during initial acute responses and in the more chronic development in tolerance. We identified key genes and pathways involved in macrophage tolerance, including the downregulation of interferon signaling. However, limitations such as the use of a single mouse strain and in vitro conditions may affect the generality of our findings. Future work should focus on validating these results in diverse models and investigating potential therapeutic interventions, such as those presented in **Table 3**, that target identified pathways to enhance macrophage function and reduce *Bb* persistence in Lyme disease.

References

1. Petnicki-Ocwieja, T., J.E. McCarthy, U. Powale, P.K. Langston, J.D. Helble, and L.T. Hu, *Borrelia burgdorferi initiates early transcriptional re-programming in macrophages that supports long-term suppression of inflammation.* PLOS Pathogens, 2023. **19**(12): p. e1011886.

2. Preventation, U.S.C.f.D.C.a. *About Lyme Disease*. 2024 [cited 2024 8/5/2024]; Available from: https://www.cdc.gov/lyme/about/index.html.

3. Bobe, J.R., B.L. Jutras, E.J. Horn, M.E. Embers, A. Bailey, R.L. Moritz, Y. Zhang, M.J. Soloski, R.S. Ostfeld, R.T. Marconi, J. Aucott, A. Ma'ayan, F. Keesing, K. Lewis, C. Ben Mamoun, A.W. Rebman, M.E. McClune, E.B. Breitschwerdt, P.J. Reddy, ..., and B.A. Fallon, *Recent Progress in Lyme Disease and Remaining Challenges.* Frontiers in Medicine, 2021. **8**.

4. Diseases, N.I.o.A.a.I. *Chronic Lyme Disease*. 2018 [cited 2018 8/5/2024].

5. Logigian, E.L., R.F. Kaplan, and A.C. Steere, *Chronic neurologic manifestations of Lyme disease.* N Engl J Med, 1990. **323**(21): p. 1438-44.

6. Davidsson, M., *The Financial Implications of a Well-Hidden and Ignored Chronic Lyme Disease Pandemic.* Healthcare, 2018. **6**(1): p. 16.

7. Hook, S.A., S. Jeon, S.A. Niesobecki, A.P. Hansen, J.I. Meek, J.K.H. Bjork, F.M. Dorr, H.J. Rutz, K.A. Feldman, J.L. White, P.B. Backenson, M.B. Shankar, M.I. Meltzer, and A.F. Hinckley, *Economic Burden of Reported Lyme Disease in High-Incidence Areas, United States, 2014-2016.* Emerg Infect Dis, 2022. **28**(6): p. 1170-1179.

8. Hirayama, D., T. Iida, and H. Nakase, *The Phagocytic Function of Macrophage-Enforcing Innate Immunity and Tissue Homeostasis.* Int J Mol Sci, 2017. **19**(1).

9. Woitzik, P. and S. Linder, *Molecular Mechanisms of Borrelia burgdorferi Phagocytosis and Intracellular Processing by Human Macrophages.* Biology (Basel), 2021. **10**(7).

10. Bockenstedt, L.K., R.M. Wooten, and N. Baumgarth, *Immune Response to Borrelia: Lessons from Lyme Disease Spirochetes.* Curr Issues Mol Biol, 2021. **42**: p. 145-190.

11. Shi, W., Z. Yang, Y. Geng, L.E. Wolinsky, and M.A. Lovett, *Chemotaxis in Borrelia burgdorferi.* J Bacteriol, 1998. **180**(2): p. 231-5.

12. Chung, Y., N. Zhang, and R.M. Wooten, *Borrelia burgdorferi elicited-IL-10 suppresses the production of inflammatory mediators, phagocytosis, and expression of co-stimulatory receptors by murine macrophages and/or dendritic cells.* PLoS One, 2013. **8**(12): p. e84980.

13. Illumina, I. *Reveal mechanisms of cell activity through gene expression analysis*. 2024 [cited 2024 8/5/2024].

14. Institute, N.C. *Gene expression profile*. 2011 [cited 2011.]

15. Korotkevich, G., V. Sukhov, N. Budin, B. Shpak, M.N. Artyomov, and A. Sergushichev, *Fast gene set enrichment analysis.* bioRxiv, 2021: p. 060012.

16. Pilarczyk, M., M. Fazel-Najafabadi, M. Kouril, B. Shamsaei, J. Vasiliauskas, W. Niu, N. Mahi, L. Zhang, N.A. Clark, Y. Ren, S. White, R. Karim, H. Xu, J. Biesiada, M.F. Bennett, S.E. Davidson, J.F. Reichard, K. Roberts, V. Stathias, A. Koleti, D. Vidovic, D.J.B. Clarke, S.C. Schürer, A. Ma'ayan, J. Meller, and M. Medvedovic, *Connecting omics signatures and revealing biological mechanisms with iLINCS.* Nature Communications, 2022. **13**(1): p. 4678.

17. Ryan, W., *willgryan/3PodR_bookdown: Pre-release for Zenodo DOI*. 2023, Zenodo.

18. Ryan V, W.G., A.S. Imami, H. Eby, J. Vergis, X. Zhan, J. Meller, R. Shukla, and R. McCullumsmith, *Interpreting and visualizing pathway analyses using embedding representations with PAVER.* Bioinformation, 2024. **20**(7): p. 700-704.

19. Miller, J.C., Y. Ma, J. Bian, K.C. Sheehan, J.F. Zachary, J.H. Weis, R.D. Schreiber, and J.J. Weis, *A critical role for type I IFN in arthritis development following Borrelia burgdorferi infection of mice.* J Immunol, 2008. **181**(12): p. 8492-503.

20. Ma, Y., K.K. Bramwell, R.B. Lochhead, J.K. Paquette, J.F. Zachary, J.H. Weis, C. Teuscher, and J.J. Weis, *Borrelia burgdorferi arthritis-associated locus Bbaa1 regulates Lyme arthritis and K/BxN serum transfer arthritis through intrinsic control of type I IFN production.* J Immunol, 2014. **193**(12): p. 6050-60.

21. Paquette, J.K., Y. Ma, C. Fisher, J. Li, S.B. Lee, J.F. Zachary, Y.S. Kim, C. Teuscher, and J.J. Weis, *Genetic Control of Lyme Arthritis by Borrelia burgdorferi Arthritis-Associated Locus 1 Is Dependent on Localized Differential Production of IFN-beta and Requires Upregulation of Myostatin.* J Immunol, 2017. **199**(10): p. 3525-3534.

22. Adler, B. and H. Adler, *Type I interferon signaling and macrophages: a double-edged sword?* Cell Mol Immunol, 2022. **19**(9): p. 967-968.

23. Krupna-Gaylord, M.A., D. Liveris, A.C. Love, G.P. Wormser, I. Schwartz, and M.M. Petzke, *Induction of Type I and Type III Interferons by Borrelia burgdorferi Correlates with Pathogenesis and Requires Linear Plasmid 36.* PLOS ONE, 2014. **9**(6): p. e100174.

24. McNab, F., K. Mayer-Barber, A. Sher, A. Wack, and A. O'Garra, *Type I interferons in infectious disease.* Nature Reviews Immunology, 2015. **15**(2): p. 87-103.

25. Information, N.C.f.B. *SLPI secretory leukocyte peptidase inhibitor [Homo sapiens (human)]*. 2024 7/31/2024 [cited 2024.

26. Zhang, S., N. Zeng, N. Alowayed, Y. Singh, A. Cheng, F. Lang, and M.S. Salker, *Downregulation of endometrial mesenchymal marker SUSD2 causes cell senescence and cell death in endometrial carcinoma cells.* PLOS ONE, 2017. **12**(8): p. e0183681.

27. Edenberg, H.J., *The genetics of alcohol metabolism: role of alcohol dehydrogenase and aldehyde dehydrogenase variants.* Alcohol Res Health, 2007. **30**(1): p. 5-13.

28. Murira, A. and A. Lamarre, *Type-I Interferon Responses: From Friend to Foe in the Battle against Chronic Viral Infection.* Frontiers in Immunology, 2016. **7**.

29. Huber, J.P. and J.D. Farrar, *Regulation of effector and memory T-cell functions by type I interferon.* Immunology, 2011. **132**(4): p. 466-74

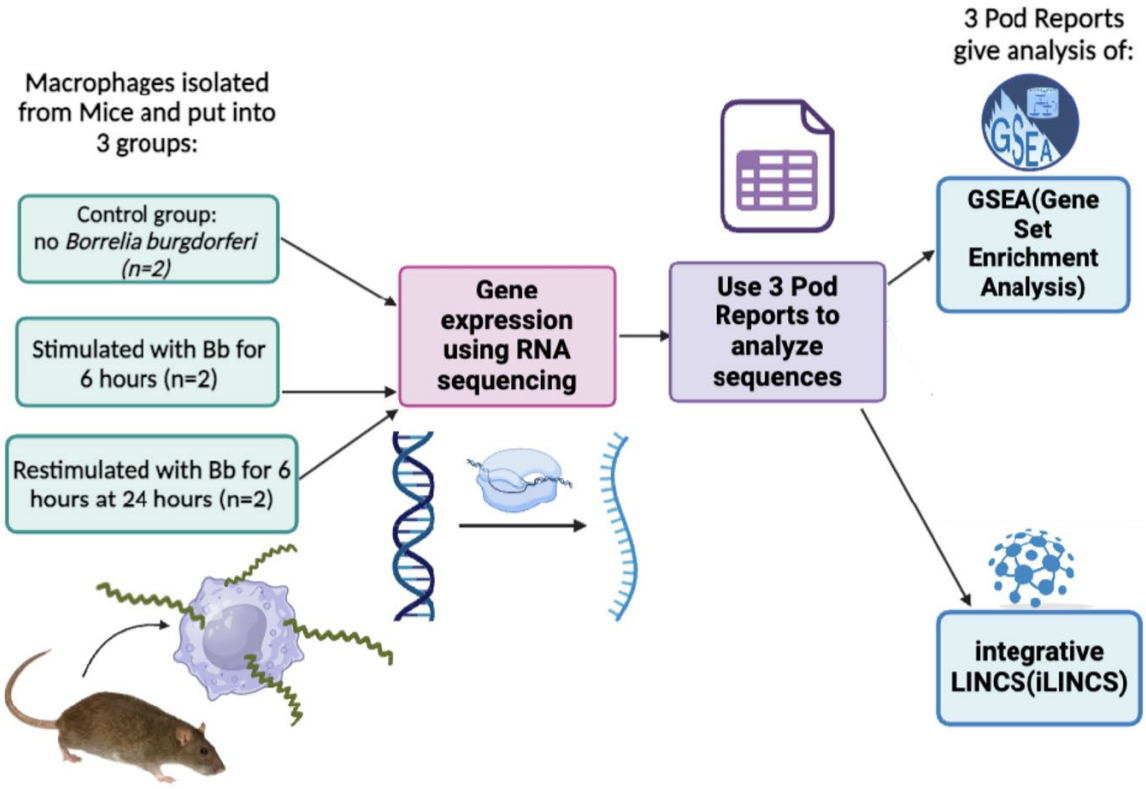

Figure 1. Workflow of the original study by Petnicki-Ocwieja et al. (1). BMDM were generated from mice and separated into three groups (n=2). The first group was a control group where no *Borrelia burgdorferi* (Bb) was administered. The second group was co-cultured with Bb for six hours. The third group was co-cultured with Bb for twenty-four hours, washed, and then restimulated for six hours before harvest. The gene expression of the macrophages was observed using RNA sequencing. Then, the differential expression results were analyzed using 3PodR and compared using GSEA and iLINCS. *Created with BioRender.com.*

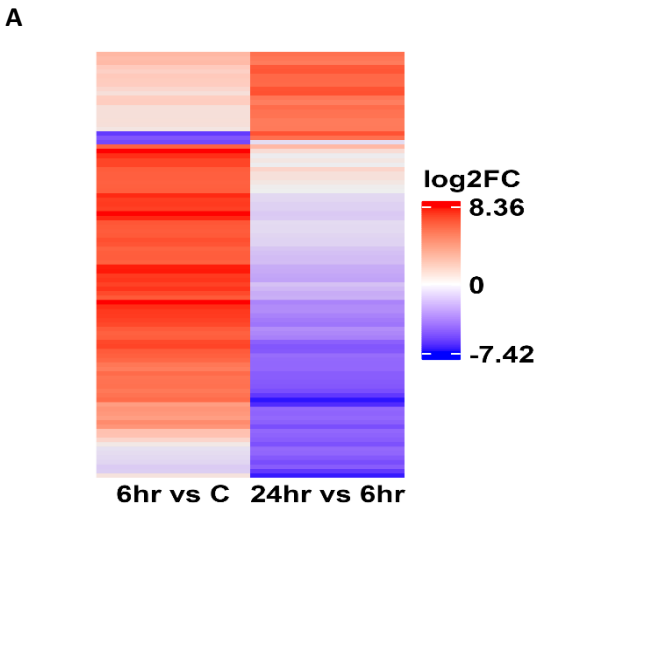

Figure 2. Heatmap displaying differentially expressed genes in stimulated and restimulated experimental groups [A]. BMDM from the 6-hour vs. control group, as well as the 24-hour vs. 6-hour group were compared to demonstrate the genes that are upregulated (red) or downregulated (blue). Volcano plots display the top upregulated and downregulated genes [B, C]. [B] depicts the top genes for the 6-hour vs. Control group, and [C] depicts the top genes for the 24-hour vs. 6-hour group.

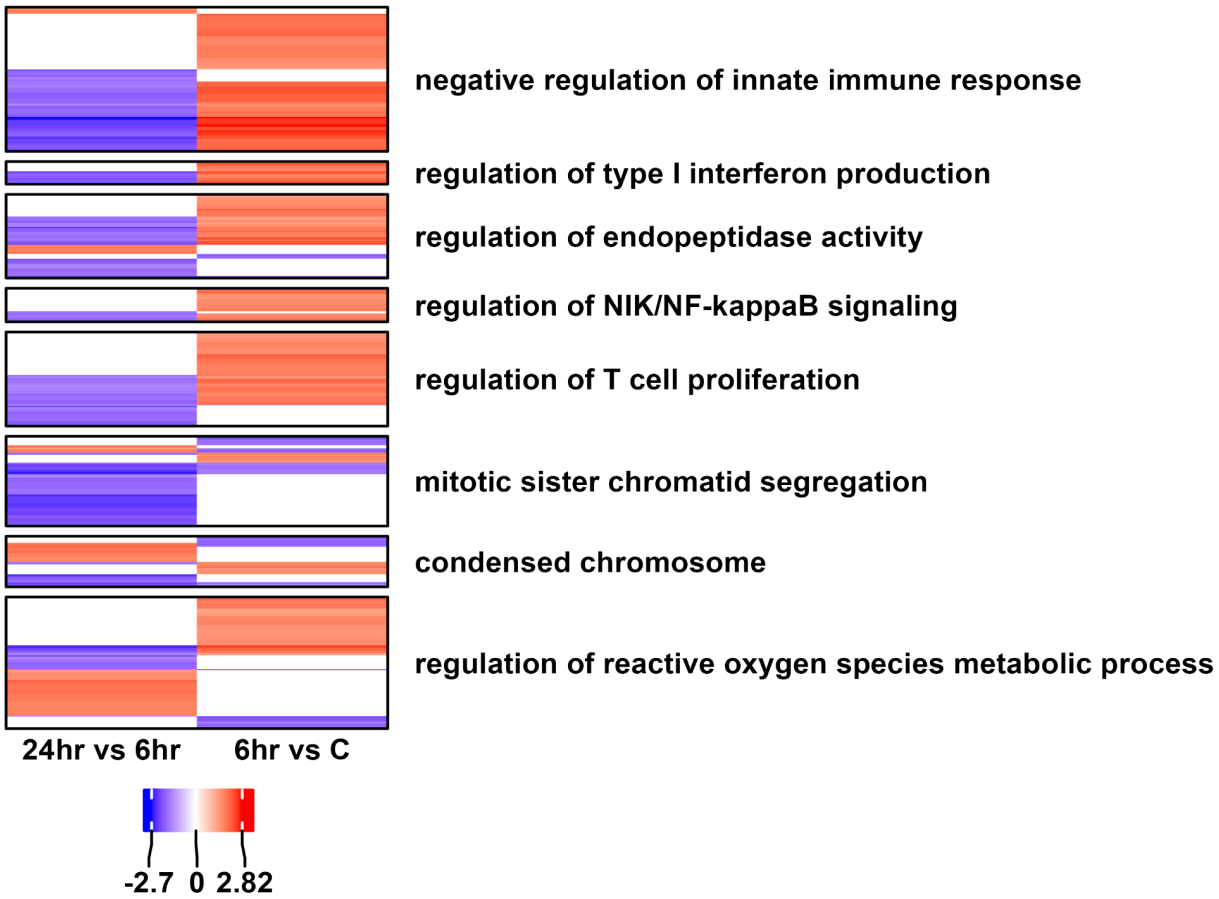

Figure 3. Heatmap displaying the PAVER clustering analysis of pathways identified as significantly dysregulated in 24hr vs 6hr or 6hr vs control groups. Rows show normalized enrichment scores (NES) of individual pathways. Clusters are annotated with PAVER-identified most representative terms.

GOID	Pathway	24hr vs 6hr	6hr vs C
GO:0001819	positive regulation of cytokine production	-2.026108965	2.541297134
GO:0032731	positive regulation of interleukin-1 beta production	-2.166431755	2.352367759
GO:0032651	regulation of interleukin-1 beta production	-2.128690795	2.291247819
GO:0032732	positive regulation of interleukin-1 production	-2.158011499	2.261213768
GO:0032652	regulation of interleukin-1 production	-2.197959624	2.200232107
GO:0032680	regulation of tumor necrosis factor production	-1.954602603	2.264451938
GO:1903555	regulation of tumor necrosis factor superfamily cytokine production	-1.949986019	2.2634614
GO:0032760	positive regulation of tumor necrosis factor production	-1.904606128	2.292463616
GO:0032479	regulation of type I interferon production	-2.084652961	2.101028638
GO:1903557	positive regulation of tumor necrosis factor superfamily cytokine production	-1.887622168	2.272065693

Table 1. Table showing select pathways in the regulation of type-I interferon production cluster. This table shows the ten highest changes in pathway dysregulation between the 6hr vs C and the 24hr vs 6hr. The table includes: the GO ID, pathway, normalized enrichment score (NES) at 24hr vs 6hr and at 6hr vs control.

Perturbagen	Similarity	MOA	Gene Targets	Cell	Tissue	Concentration	Time	FDA Phase
PHA-793887	0.65	CDK inhibitor	CDK1|CDK10|CDK11B|CDK12|CDK13|CDK14|CDK15|CDK16|CDK17|CDK18|CDK19|CDK2	BT20	breast	3.33uM	24h	1
Palbociclib	0.632	CDK inhibitor	CCND1|CDK4|CDK6	MDAMB231		10uM	24h	4
Cladribine	0.631	Adenosine deaminase inhibitor	ADA	VCAP	prostate	10uM	6h	4
Pevonedistat	0.626	Nedd activating enzyme inhibitor	NAE1|UBA3	HELA	large intestine	1.11uM	24h	2
O-Demethylated Adapalene	0.609	Retinoid receptor agonist	RARG	VCAP	prostate	10uM	6h	
Gemcitabine	0.598	Ribonucleotide reductase inhibitor	POLA1|POLD1|POLE|RRM1|RRM2|RRM2B	VCAP	prostate	0.1uM	6h	4
Wortmannin	0.598	PI3K inhibitor	PIK3CA|PIK3CG|PLK1	VCAP	prostate	10uM	24h	
Fludarabine	0.595	DNA synthesis inhibitor	RRM1	VCAP	prostate	10uM	6h	
CGK733	0.585	ATM kinase inhibitor|ATR kinase inhibitor	ATM|ATR	HUVEC	umbilical vein	10uM	24h	
Niclosamide	0.583	DNA replication inhibitor|STAT inhibitor	STAT3	HT29	large intestine	10uM	24h	4

Table 2. Top LINCS Concordant Signatures for 24 hr vs 6hr groups. Top concordant chemical perturbagens from the LINCS database, potentially enhancing macrophage tolerance effects induced by *Borrelia burgdorferi*.

Perturbagen	Similarity	MOA	Gene Targets	Cell	Tissue	Concentration	Time	FDA Phase
SCHEMBL1564574	-0.576	CHK inhibitor	CHEK1|CHEK2	MCF7	breast	1uM	6h	
VU0365118-1	-0.505			VCAP	prostate	10uM	24h	
Parbendazole	-0.501	Tubulin inhibitor	TUBB	VCAP	prostate	0.5uM	24h	
MLS000925170	-0.499			VCAP	prostate	10uM	24h	
CHEMBL3188661	-0.495	DDR1 inhibitor	DDR1	ASC.C		1.11uM	24h	
Docetaxel Intermediate	-0.492	Tubulin inhibitor	TUBB	VCAP	prostate	10uM	24h	
Podofilox	-0.49	Microtubule inhibitor|Tubulin inhibitor		VCAP	prostate	10uM	24h	4
ZINC01792951	-0.49			VCAP	prostate	10uM	24h	
Tivantinib	-0.483	Tyrosine kinase inhibitor	MET	NPC	neural progenitor cells	1.11uM	24h	3
Triazolothiadiazine, 9	-0.483	Phosphodiesterase inhibitor		VCAP	prostate	10uM	24h	

Table 3. Top LINCS Discordant Signatures for 24 hr vs 6hr groups. Top discordant chemical perturbagens identified in the LINCS database, potentially reversing macrophage tolerance effects induced by *Borrelia burgdorferi*.

